THE THEORY, DESIGN, AND PERFORMANCE OF A TWO DIMENSIONAL HIGH SPEED, INDUCTION TYPE, WIND TUNNEL

Thesis by

Lt. Comdr. R. F. Kane, USN

and

E. F. Kelley

In Partial Fulfillment of the Requirements for the Professional Degree in Aeronautical Engineering

California Institute of Technology

Pasadena, California

1943

ACKNOWLEDGEMENT

The authors are deeply indebted to Mr. A. E. Puckett of GALCIT for his invaluable assistance, cooperation and advice in the development of this project and in the preparation of this paper.

R. F. Kane

E. F. Kelley

California Institute of Technology
Pasadena, California
May 27, 1943

TABLE OF CONTENTS

NOTATION

M = Mach Number (= u/a)

λ = Compression ratio

r = A_j/A_3 = Jet Area/Working Section Area

m = Mass flow per unit time

p = Static pressure (absolute)

u = Velocity

A = Area

ρ = Density

η = Efficiency

γ = c_p/c_v = 1.405

a = Local speed of sound

a^* = Speed of sound at point where M = 1

SUBSCRIPTS

$( )_1$ = Refers to working section

$( )_2$ = " " jet exit

$( )_3$ = " " mixing section

$( )_4$ = " " diffuser exit (atmosphere)

$( )_j$ = " " jet throat

$( )_s$ = " " motive air before expansion

SUMMARY

(1) A two-dimensional wind tunnel, induction type, of rectangular working section, 2 1/2" x 12", has been designed and constructed for the purpose of testing aerodynamic shapes at velocities close to the speed of sound.

(2) The design theory is based upon the fundamental equations of momentum, continuity, and energy with the assumptions that mixing takes place at constant area and that jet exit velocities in the supersonic range may be obtained.

(3) Calibration runs, in which the maximum Mach number of 0.65 was obtained, revealed that the actual tunnel performance did not agree with the design performance curves except at high compression ratios.

(4) A variation of the original theory, i.e., sonic jet exit velocities, was used to obtain a new set of design curves. These curves are in excellent agreement with actual performance data except at high compression ratios.

(5) Failure of the tunnel to meet design conditions is considered to lie in the jet shape which assumes a true supersonic nozzle shape only at small jet openings (high compression ratios).

INTRODUCTION

In order to study the flow of air about aerodynamic shapes at velocities approaching a Mach number of one, it is essential that the working section flow be as smooth as possible, and free from the unstable fluctuations common to wakes from air screws or jets. The induction type tunnel allows such a flow through the working section, and also increases the mass flow available over that of the supply of motive air, thereby greatly increasing the dimensions of the working section possible with a given air supply installation.

The tunnel in general consists of six essential parts, the converger or induction air orifice, working section, motive air jet, mixing section, diffuser; and measuring or recording apparatus.

The converger acts as an orifice for the working section, increasing the effective cross-section area, thereby reducing any nozzle loss that might otherwise result in power consumption at this point.

The working section should be transparent, and devices must be incorporated to measure the reactions of the model being tested. At velocities approaching a Mach number of one the size of the model is greatly restricted by the sensitiveness of such flow to small changes in net throat area, and, to that end, flexible boundaries are employed to maintain a constant net throat area, thus maintaining a satisfactorily steady flow.

The motive air jet must be designed to give super-sonic flow (at the jet exit) for practical operating conditions, and in this tunnel the jet area is adjustable, which allows a considerable range of operating head pressures before the jet. This condition allows some control of working

section speed, but a change in mass flow of motive air results in more reaction by the induced flow. The function of the jet, then, is to supply kinetic energy to the apparatus at super-sonic velocities, and in an optimum direction.

Entrainment and mixing between the motive and induced flows take place in the mixing section. The equations resulting in the performance and design curves are based upon conceptions of what takes place in this section. It is assumed that mixing takes place at constant area in these calculations.

The diffuser converts the dynamic energy of the mixing section to potential energy, thereby retaining this energy in the cycle with a minimum of loss due to turbulence and non-uniform flow in general.

Visual air flow is developed using the Schlieren optical method. A strong light source supplies rays to a system of mirrors which direct the rays through the glass-walled working section, and finally to an adjustable, knife-edge, aperture located at the focal point of one mirror. Any deviation of density in the working section due to a compressibility effect causes a slight refraction of some of the light passing to the knife edge. By adjusting this edge, these rays are eliminated from the beam, and a corresponding difference in light intensity is recorded on parts of the visual screen beyond, thereby producing a picture of the wave pattern taking place at the model. An overhead beam is provided which supports the mirrors, controls, screen, and other pertinent equipment. This beam is mounted on rails and can be raised and lowered so that any part of the working section can be effectively investigated.

At the present time, the initial development work on the tunnel is still in progress and no models as yet have been tested in the tunnel.

S E C T I O N 1

THEORY

(A) Supersonic Jet Theory

(B) Sonic Jet Theory

(A) SUPERSONIC JET THEORY AND DEVELOPMENT OF EQUATIONS:

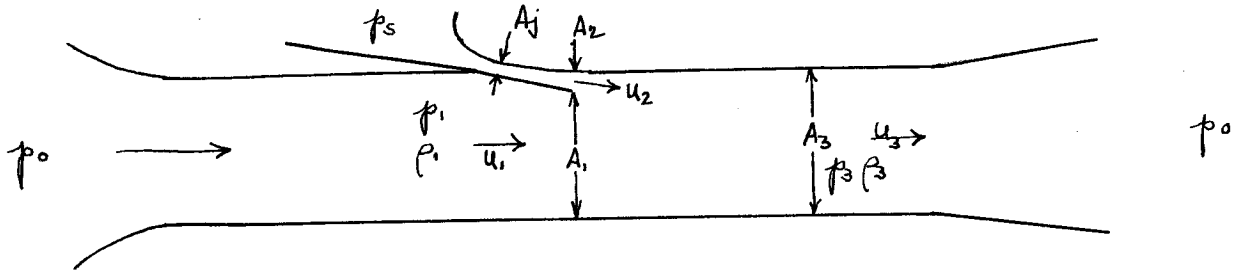

The design curves are derived from the development of three fundamental equations; the continuity equation,

$$A_3u_3\rho_3 = A_2u_2\rho_2 + A_1u_1\rho_1$$

the momentum equation,

$$A_3(p_1-p_3) = A_3\rho_3u_3^2 - (A_2\rho_2u_2^2 + A_1\rho_1u_1^2)$$

and the energy equation,

$$\left(\frac{u_3^2}{2} + \frac{\gamma}{\gamma-1}\frac{p_3}{\rho_3}\right)\rho_3u_3A_3=\left(\frac{u_2^2}{2} + \frac{\gamma}{\gamma-1}\frac{p_2}{\rho_2}\right)\rho_2u_2A_2+\left(\frac{u_1^2}{2}+\frac{\gamma}{\gamma-1}\frac{p_1}{\rho_1}\right)\rho_1u_1A_1$$

Assuming the temperature is the same for both the motive air supply and induced air intake at the tunnel, the energy equation is thereby simplified, and

$$\frac{\gamma}{\gamma-1}\frac{p_1}{\rho_1} + \frac{u_1^2}{2} = \frac{\gamma}{\gamma-1}\frac{p_2}{\rho_2} + \frac{u_2^2}{2}$$

(In the appendix the letter "C" is used to indicate the sum of these total energies.)

Since the terminal conditions of the induced flow, the design condition of induced flow in the working section, and the state of the motive fluid before expansion, are either known, or specified, the solution for ρ_3,u_3 and p_3 from these three equations gives the other conditions in the system necessary for the attainment of the design conditions.

Using the momentum equation, eliminating ρ_3 by substitution of of its value through relations in the continuity equation, and by making the transformations shown in the appendix, an equation of $p_3/p_1$is finally

obtained as a function of areas A_2/A_1, and Mach numbers, M_1 and M_2. Through the assumption of constant area mixing, $A_1 + A_2 = A_3$.

From the energy equation an expression for u_3 is obtained in terms of A_3, p_3, m_1 and m_2, and, introducing ρ_1 in both numerator and denominator, and using the relations of the continuity equation, u_3 is obtained as a function of p_3/p_1, A_2/A_1, ρ_1, u_1, ρ_2, u_2, and a*. By dividing through with a* the terms are further reduced to M_1, M_2, p_3/p_1 and u/a^*.

Since p_3/p_1 has already been reduced to a calculable equation, and M_1, M_2, and A_2/A_1 are to be selected as arbitrary combinations for a final graphical solution, this leaves u/a^* to be determined. U/a^* is a function of M , as shown in Fig. 1.6.

From the De Laval nozzle equation for a compressible fluid, relations of p_4/p_3 and p_1/p_o are determinable. An overall efficiency factor p_4/p_o is then the product of $p_4/p_3 \times p_3/p_1 \times p_1/p_o$, and is equal to unity for a theoretical design condition of no losses. In the p_4/p_3 factor, an efficiency of $\eta = 75\%$ is introduced to cover the diffuser losses, and later a p_4/p_o design condition of 1.05 is used, instead of 1.0 to include friction losses in the working and mixing sections of the tunnel. Again using the Laval equation, λ (compression ratio) is calculated as a function of M_1 and M_2 thereby reducing by one the number of parameters involved.

The curves of Figs. 1.2 - 1.5 inclusive are now drawn by selecting a set of λ's $[= f(M_1, M_2)]$ for pertinent values of working section Mach numbers, and incorporating several values of A_2/A_1 (or A_j/A_3) for each λ. A value of p_3/p_1 is first calculated from these parameters, and then introduced in the equation for u_3/a^* together with the same parameters.

With this value of u_3/a^*, M_3 is selected from Fig. 1.6, and this allows an evaluation of p_4/p_3. The value of p_4/p_o is then calculated as described above and plotted vs. A_j/A_3 for a set of λ's for each selected M_1.

In transferring the data from Fig. 1.2 - 1.5, inclusive, to Fig. 1.1 an efficiency is assigned the working and mixing sections by considering the intersection of $p_4/p_o = 1.05$ with the λ curves.

Fig. 1.1 is plotted incorporating the λ vs. M_1 relations for various values of A_j/A_3 at the design condition of $p_4/p_o = 1.05$. For a given area ratio between motive air nozzle and working section area the necessary λ is indicated for the desired Mach number in the working section.

Now by calculating the λ's that the various nozzle areas will establish with the compressor capacity available another curve may be drawn on Fig. 1.1, and where this curve crosses an A_j/A_3 curve at the desired working section Mach number, the operating conditions are determined.

This concludes the theoretical determination of an operating condition from these original three equations using the given assumptions, particularly that the mixing takes place in a constant area, that M_2 is a true function of λ and is not affected by other considerations such as disturbing shock waves.

A complete algebraic treatment of the equations and calculations is included in the appendix.

(B). SONIC JET THEORY

The vital condition in the "Supersonic Jet Theory", that of obtaining supersonic speeds in the motive air supply after emergence from the nozzle throat, is one which easily might not be attainable in an actual induction tunnel because of critical nature of supersonic flows.

Accordingly, the constant area mixing theory was applied, not at the nozzle exit as in the Supersonic Jet Theory, but at the nozzle throat, and calculations were made so as to predict the theoretical performance of an induction type tunnel operating under this condition, i.e,. a Sonic Jet.

A concise theatment of the theory follows immediately together with a plot of the theoretical performance, (fig. 1.10). The calculations are included in the appendix.

SONIC JET THEORY

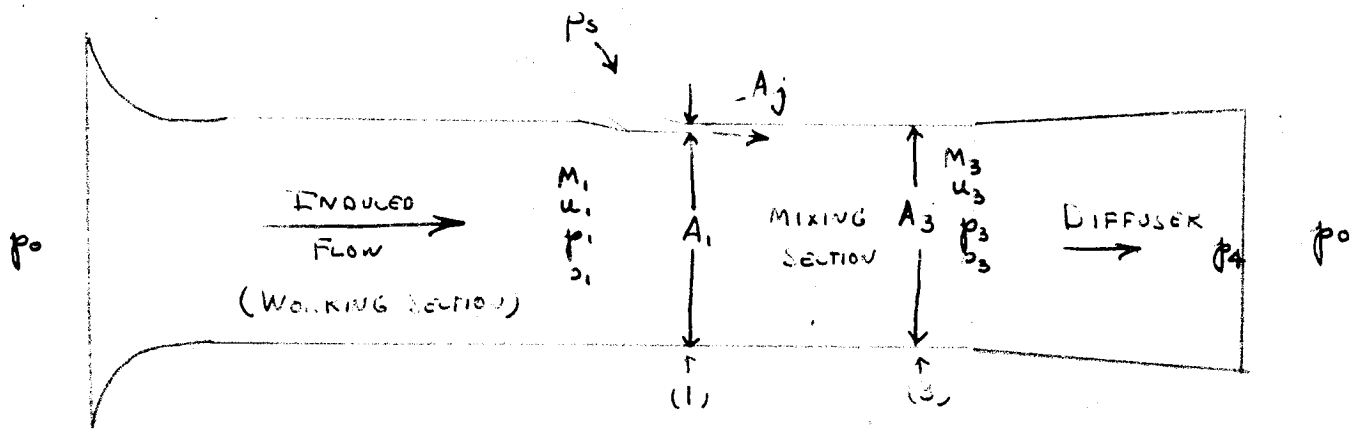

$$A_1 + A_j = A_3 = \text{WORKING SECTION AREA}$$

BETWEEN POINTS (1) AND (3) IN SKETCH ABOVE:

(1) $m_3 u_3 - m_1 u_1 - m_j u_j = p_1 A_1 + p_j A_j - p_3 A_3$ (MOMENTUM Eq.)

(2) $\rho_1 u_1 A_1 + \rho_j u_j A_j = \rho_3 u_3 A_3$ (CONTINUITY Eq.)
$(m_1 + m_j = m_3)$

(3) $\left(\frac{1}{2} u_1^2 + \frac{\gamma}{\gamma-1} \frac{p_1}{\rho_1}\right) m_1 + \left(\frac{1}{2} u_j^2 + \frac{\gamma}{\gamma-1} \frac{p_j}{\rho_j}\right) m_2 =$
$= \left(\frac{1}{2} u_3^2 + \frac{\gamma}{\gamma-1} \frac{p_3}{\rho_3}\right) m_3$ (ENERGY Eq.)

ASSUMING THAT STAGNATION TEMPERATURE (T_o) IS THE SAME FOR BOTH THE SUPPLY AND THE INDUCED AIR, AND NOTING THAT THE JET IS SUCH (CONVERGENT NOZZLE) THAT $M=1$ AND THEREFORE p_j AND ρ_j ARE FUNCTIONS OF THE SUPPLY PRESSURE (p_s) ALONE, THE ABOVE EQUATIONS GIVE:

(4) $$\frac{p_3}{p_1} = \frac{1}{1+\gamma}\left[\frac{A_1}{A_3}\left(1+\gamma M_1^2\right) + \frac{A_j}{A_3}\frac{p_j}{p_1}(1+\gamma)\right] +$$
$$+ \sqrt{\left(\frac{\gamma}{\gamma+1}\right)^2 [\;\;]^2 - \gamma^2\left(\frac{A_1}{A_3}\frac{M_1^2}{\frac{u_1^2}{a^*}} + \frac{A_j}{A_3}\frac{p_j}{p_1}\right)^2}$$

↑ Same as term immediately above 1.5 in similar brackets.

Equation (4) above was obtained in exactly the same manner as the corresponding equation in the "SUPERSONIC" JET THEORY immediately preceding.

FROM the ENERGY Eq. (3), we obtain:

$$(5)\quad \frac{u_3}{a^*} = \left[\frac{1}{1-\gamma}\left(\frac{p_3}{p_1}\right)\frac{1+\frac{A_2}{A_1}}{\frac{M_1^2}{\frac{u_1}{a^*}}+\frac{A_2}{A_1}}\right] + \sqrt{\left[\quad\right]^2 + \frac{\gamma+1}{\gamma-1}}$$

(Same)

and

$$(6)\quad \frac{p_4}{p_3} = \left(1+\frac{\gamma-1}{2}M_3^2\right)^{\frac{\gamma\eta}{\gamma-1}} \quad \text{(Isentropic Process)}$$

where η = DIFFUSER EFFICIENCY

Finally

$$(7)\quad \frac{p_4}{p_0} = \frac{p_4}{p_3}\cdot\frac{p_3}{p_1}\cdot\frac{p_1}{p_0}$$

- The calculations were carried out in the same manner as in the "SUPERSONIC JET THEORY". The diffuser efficiency (η) was assumed to be the same value (75%), and friction losses were taken into consideration by assuming $p_4/p_0 = 1.05$

Kane_rf_1943
Melley_ef_1943

$r \rightarrow$ .13 .12 .11 .10 .09 .08 .07 .06 .05 .04 .03 .02

M_1

MACH NO. WORKING SECTION

1.1
1.0
0.9
0.8
0.7
0.6
0.5
0.4
0.3
0.2
0.1
0

1 2 3 4 5 6 7

λ (= Compression Ratio)

THEORETICAL PERFORMANCE CURVES
INDUCTION WIND TUNNEL
- SUPERSONIC JET -

$r = \frac{A_j}{A_3} = \frac{\text{JET AREA}}{\text{WORKING SECT. AREA}}$

FIG. 1.1

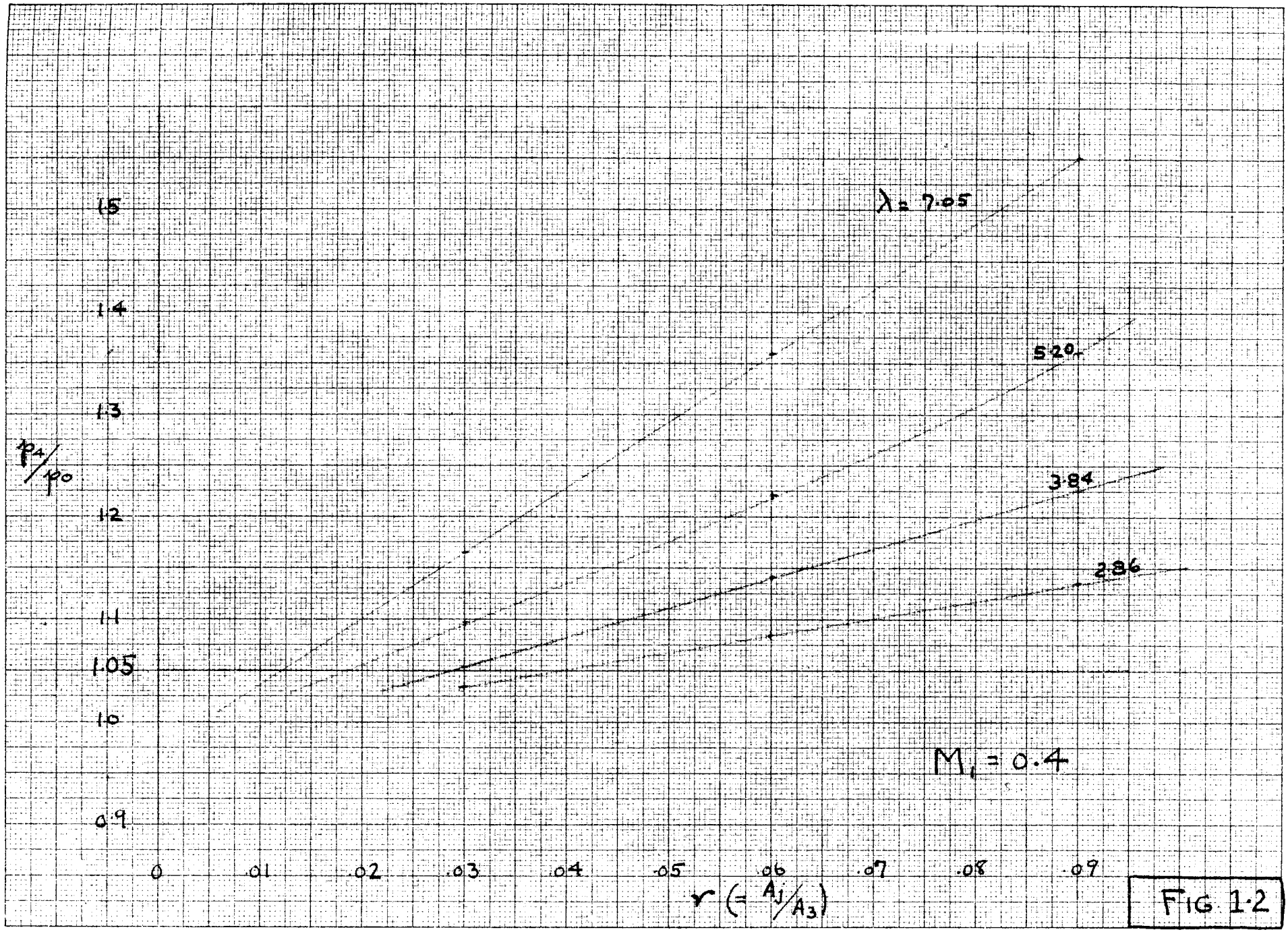
λ = 7.05
5.20
3.84
2.86
M₁ = 0.4
p4/p0
1.5
1.4
1.3
1.2
1.1
1.05
1.0
0.9
0
.01
.02
.03
.04
.05
.06
.07
.08
.09
r (= Aj/A3)

FIG 1·2

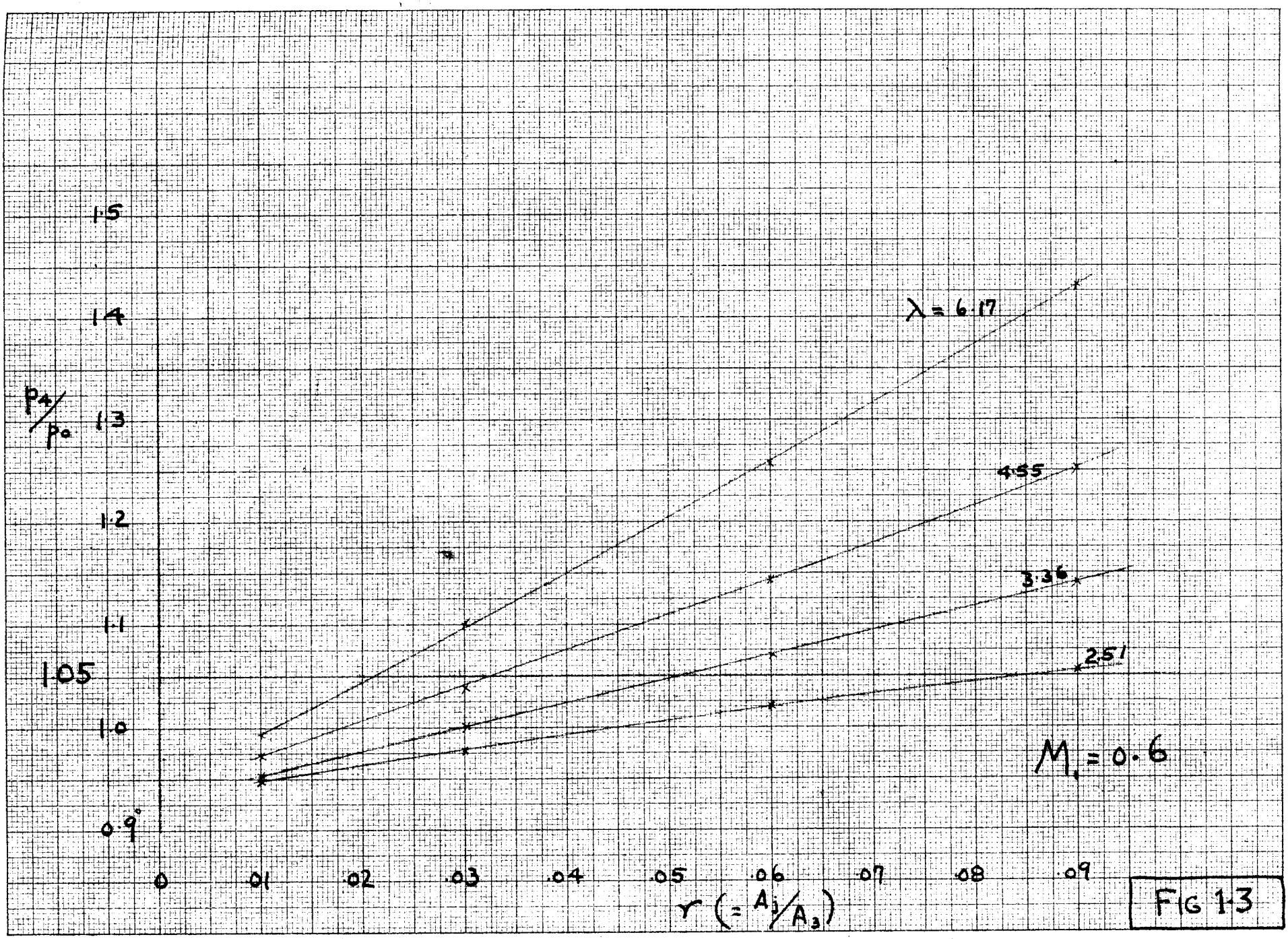
1·5
1·4
1·3
1·2
1·1
1·05
1·0
0·9
P4/P0
λ = 6·17
4·55
3·36
2·51
M1 = 0·6
0
·01
·02
·03
·04
·05
·06
·07
·08
·09
r (= A3/A3)

FIG 1·3

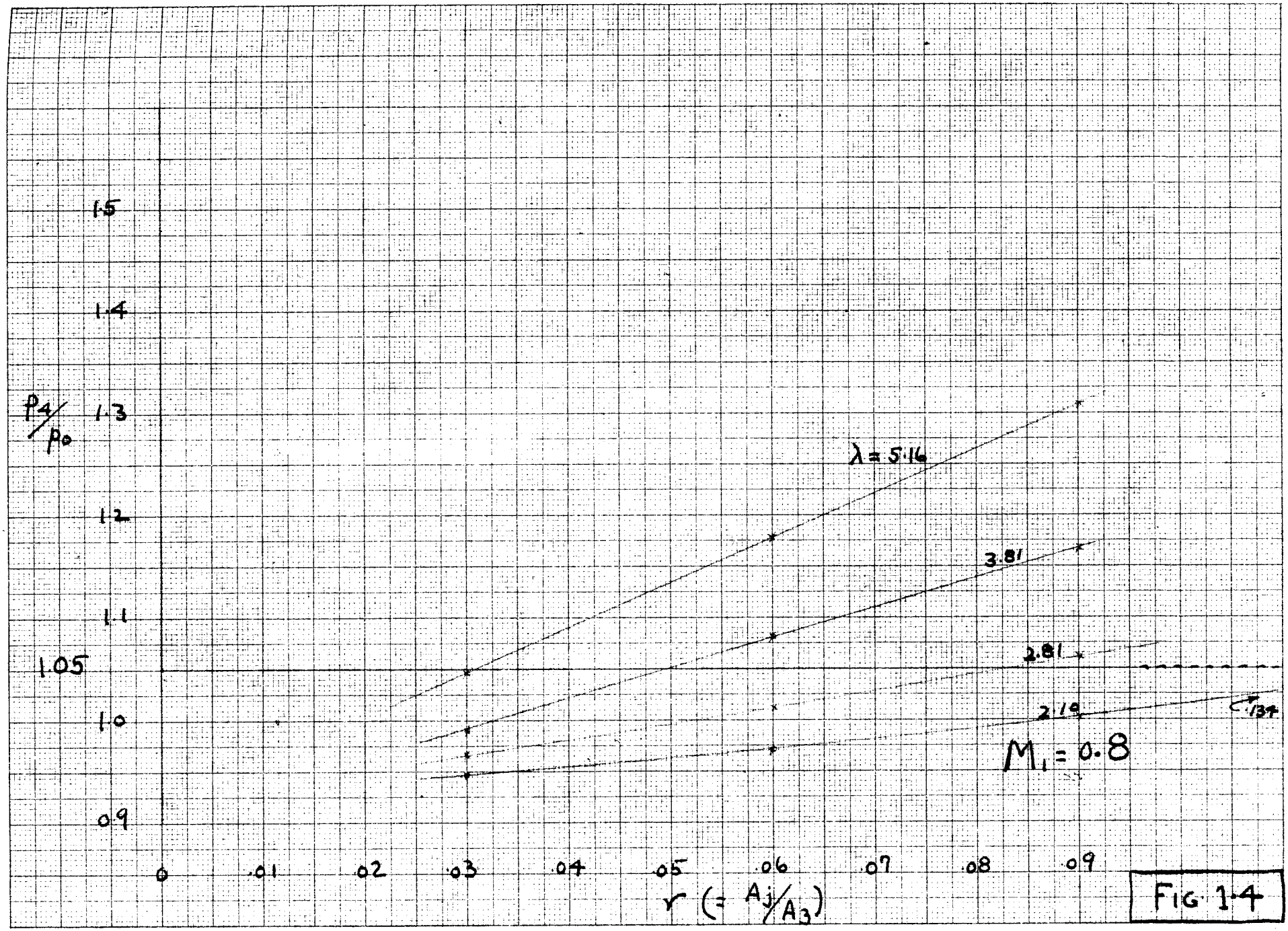
1.5
1.4
P_1/P_0
1.3
1.2
1.1
1.05
1.0
0.9
0
.01
.02
.03
.04
.05
.06
.07
.08
.09
r (= A_j/A_3)
λ = 5.16
3.81
2.81
2.19
1.37
$M_1 = 0.8$

FIG 1.4

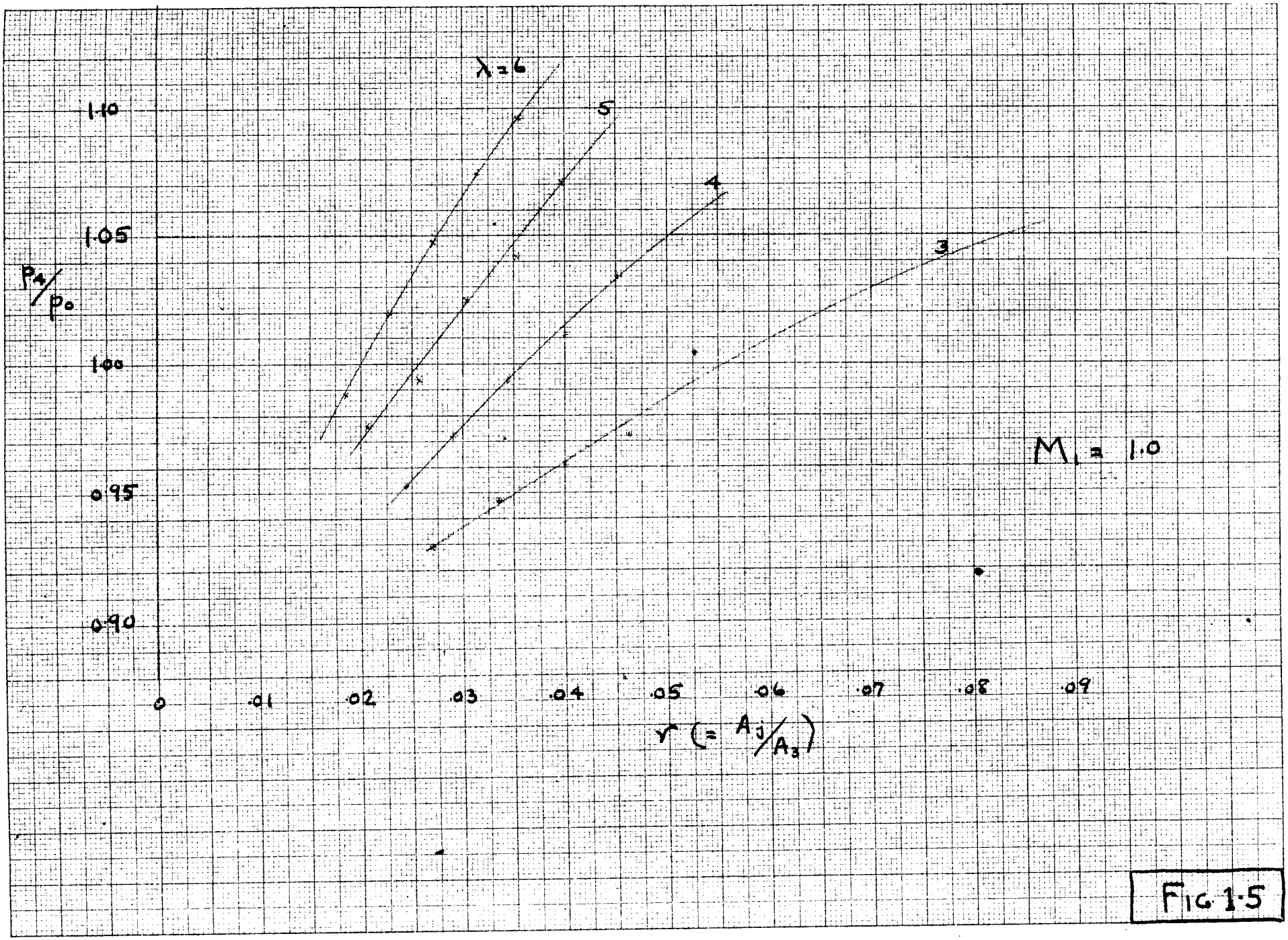
λ=6
5
4
3
1.10
1.05
1.00
0.95
0.90
P4/P0
M1 = 1.0
0
.01
.02
.03
.04
.05
.06
.07
.08
.09
r (= Aj/A3)

FIG 1.5

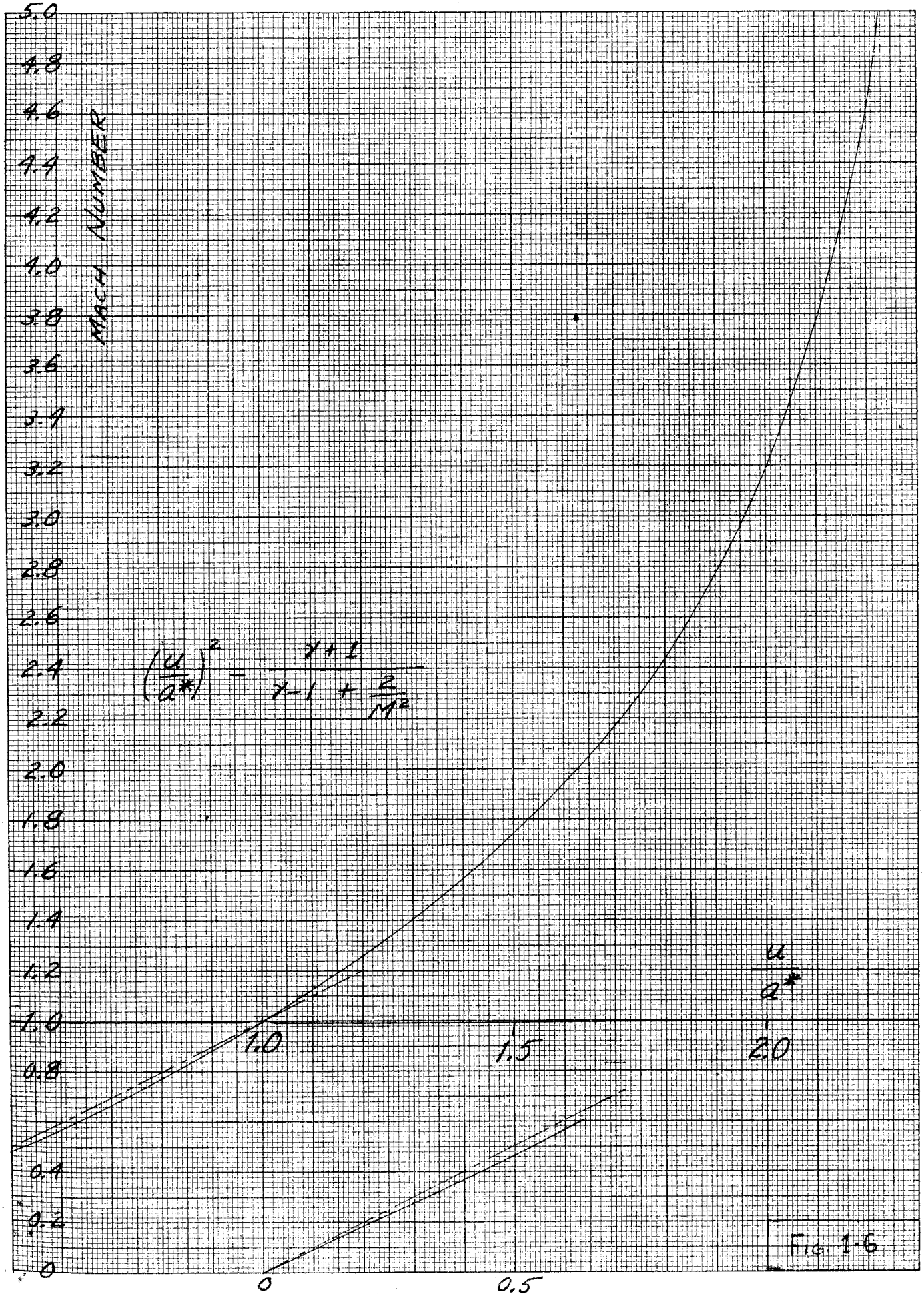
MACH NUMBER
5.0
4.8
4.6
4.4
4.2
4.0
3.8
3.6
3.4
3.2
3.0
2.8
2.6
2.4
2.2
2.0
1.8
1.6
1.4
1.2
1.0
0.8
0.4
0.2
0
0
0.5
1.0
1.5
2.0
u/a*
$\left(\frac{u}{a^*}\right)^2 = \frac{\gamma+1}{\gamma-1+\frac{2}{M^2}}$

Fig. 1-6

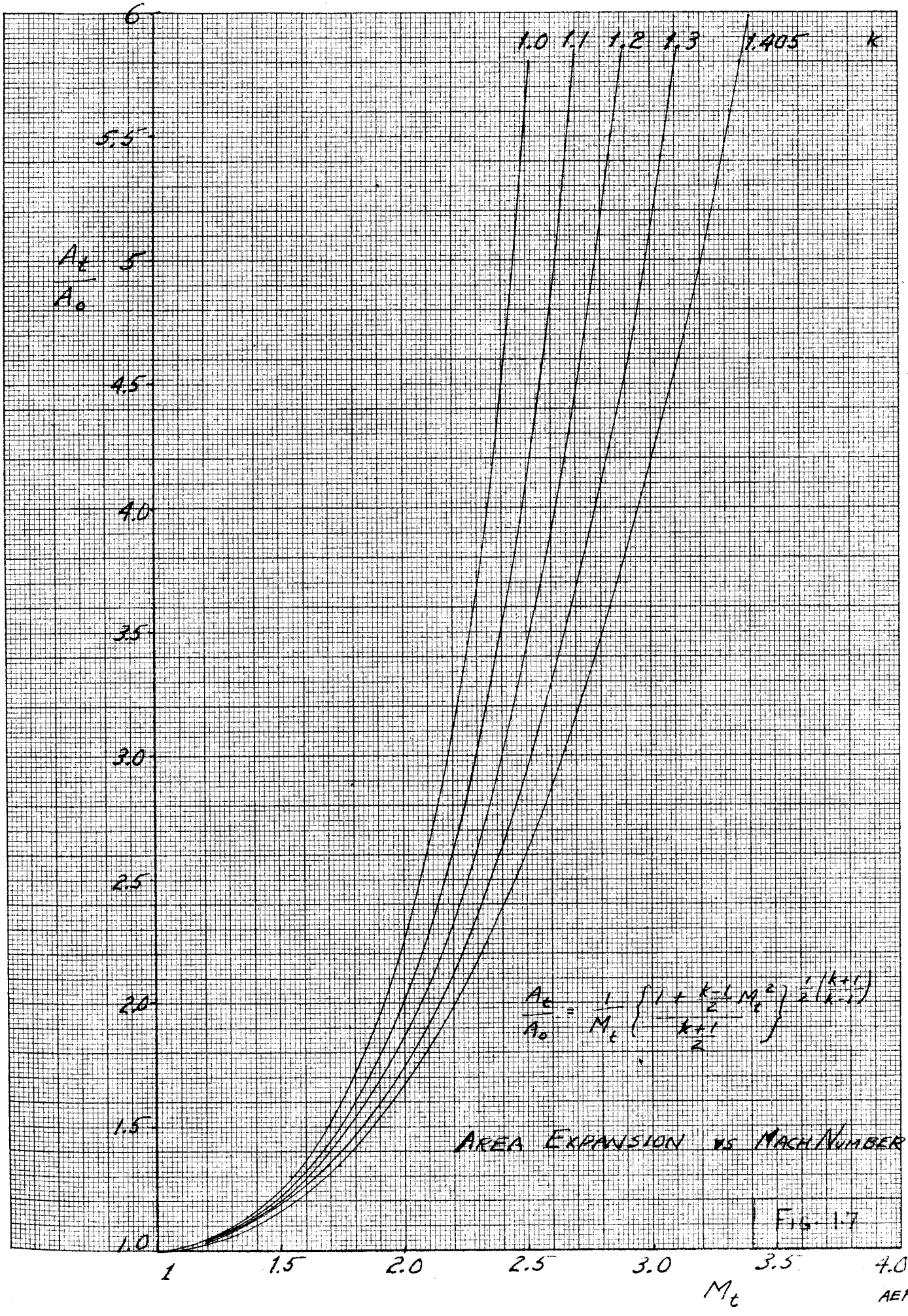
6
5.5
5
4.5
4.0
3.5
3.0
2.5
2.0
1.5
1.0
$\frac{A_t}{A_0}$
1.0 1.1 1.2 1.3 1.405 k
1
1.5
2.0
2.5
3.0
3.5
4.0
M_t
$\frac{A_t}{A_0} = \frac{1}{M_t}\left(\frac{1+\frac{k-1}{2}M_t^2}{\frac{k+1}{2}}\right)^{\frac{1}{2}\left(\frac{k+1}{k-1}\right)}$
AREA EXPANSION vs MACH NUMBER
FIG. 1.7
AEP

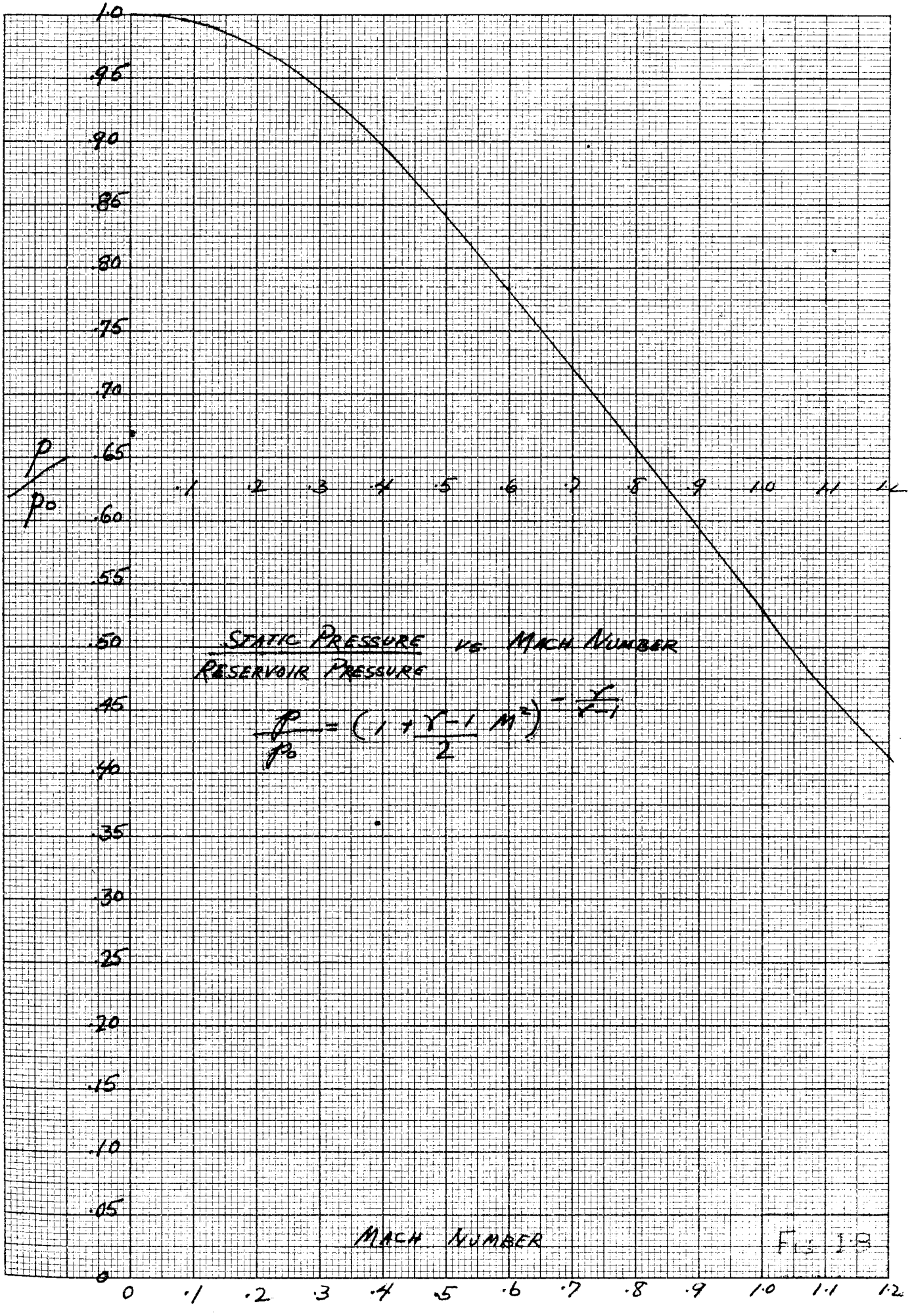
1.0
.95
.90
.85
.80
.75
.70
.65
.60
.55
.50
.45
.40
.35
.30
.25
.20
.15
.10
.05
0
p/p0
.1 .2 .3 .4 .5 .6 .7 .8 .9 1.0 1.1 1.2
STATIC PRESSURE / RESERVOIR PRESSURE vs. MACH NUMBER
p/p0 = (1 + (γ−1)/2 M²)^(−γ/(γ−1))
MACH NUMBER
0 .1 .2 .3 .4 .5 .6 .7 .8 .9 1.0 1.1 1.2

FIG. 1B

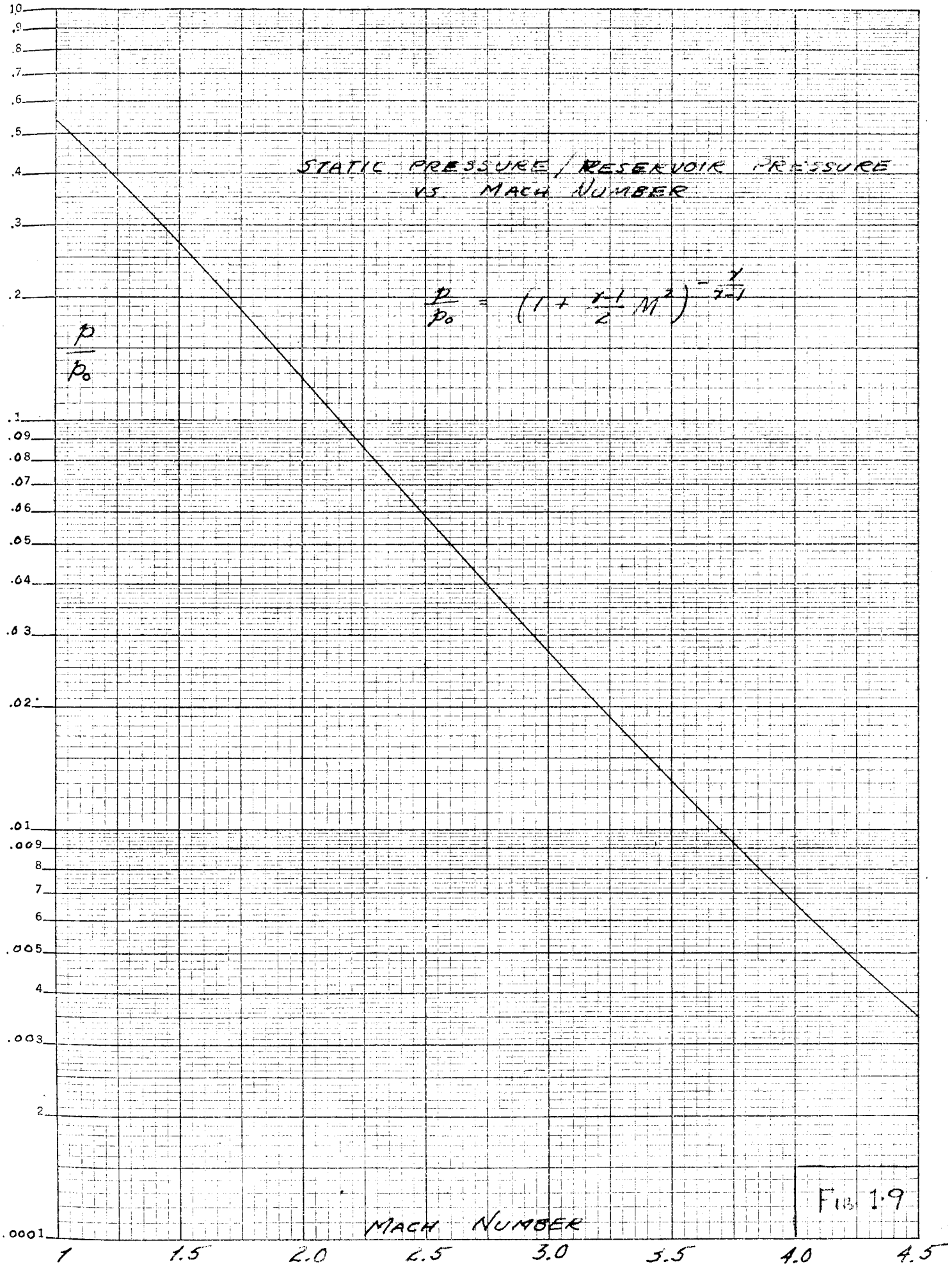
STATIC PRESSURE / RESERVOIR PRESSURE
VS. MACH NUMBER
$\frac{p}{p_0} = \left(1 + \frac{\gamma-1}{2} M^2\right)^{-\frac{\gamma}{\gamma-1}}$
$\frac{p}{p_0}$
10
.9
.8
.7
.6
.5
.4
.3
.2
.1
.09
.08
.07
.06
.05
.04
.03
.02
.01
.009
8
7
6
.005
4
.003
2
.0001
1
1.5
2.0
2.5
3.0
3.5
4.0
4.5
MACH NUMBER

FIG 1.9

Kline_et_1943
Kelley_et_1943

M_2 = MACH NUMBER - WORKING SECTION

1.0
0.9
0.8
0.7
0.6
0.5
0.4
0.3
0.2
0.1
0

r → .19 .18 .17 .16 .15 .14 .13 .12 .11 .10 .09 .08 .07 .06 .05 .04 .03 .02

1 2 3 4 5 6 7

λ = COMPRESSION RATIO

THEORETICAL PERFORMANCE CURVES
INDUCTION WIND TUNNEL
CONSTANT AREA MIXING
SONIC JET ($M = 1$)

$r = \frac{A_j}{A_3} = \frac{\text{JET AREA}}{\text{MIXING AREA}}$

FIG. 1-10

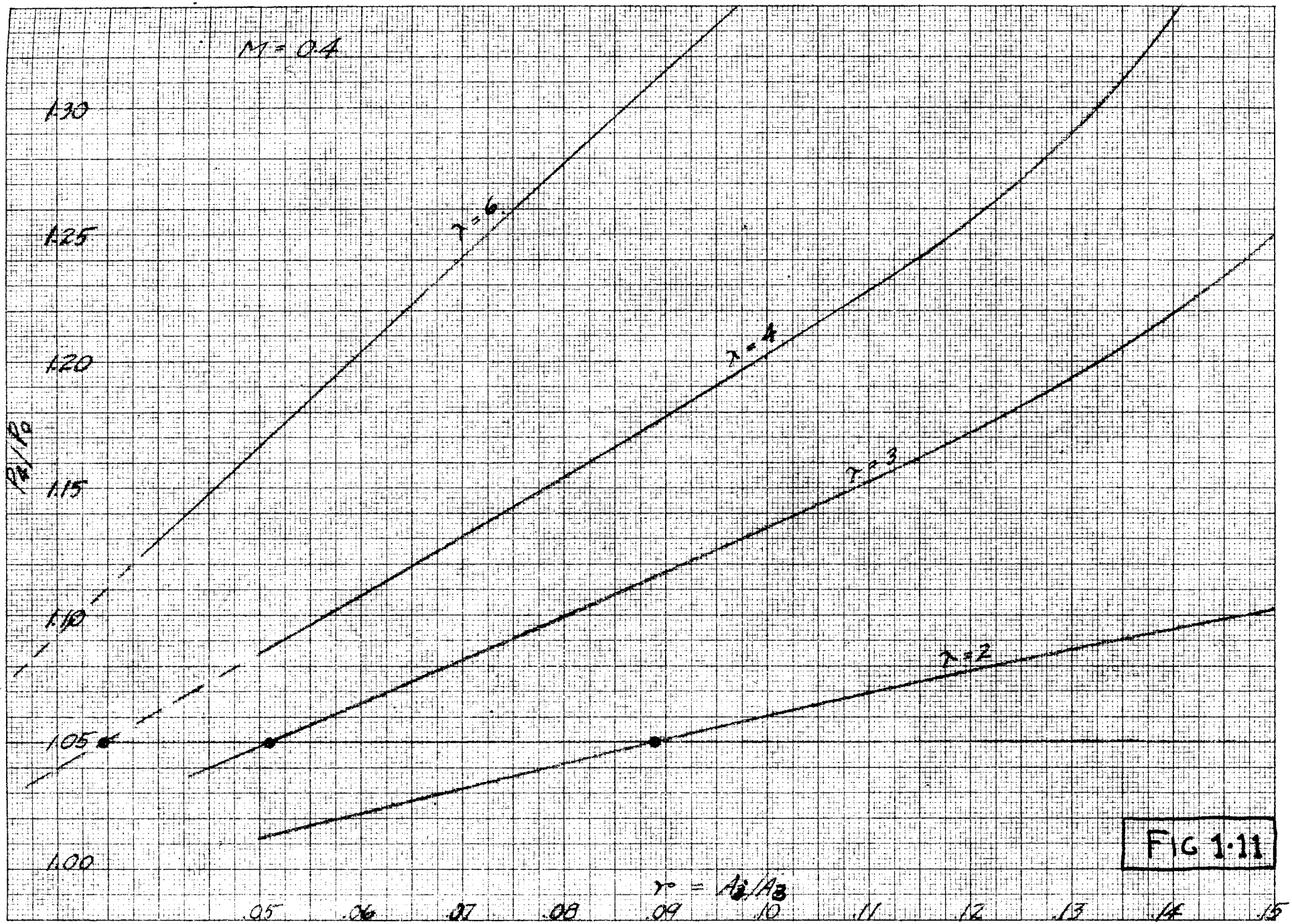
M = 0.4
1.30
1.25
1.20
1.15
1.10
1.05
1.00
P1/P0
γ = 6
γ = 4
γ = 3
γ = 2
.05
.06
.07
.08
.09
.10
.11
.12
.13
.14
.15
γ = A2/A3

FIG 1.11

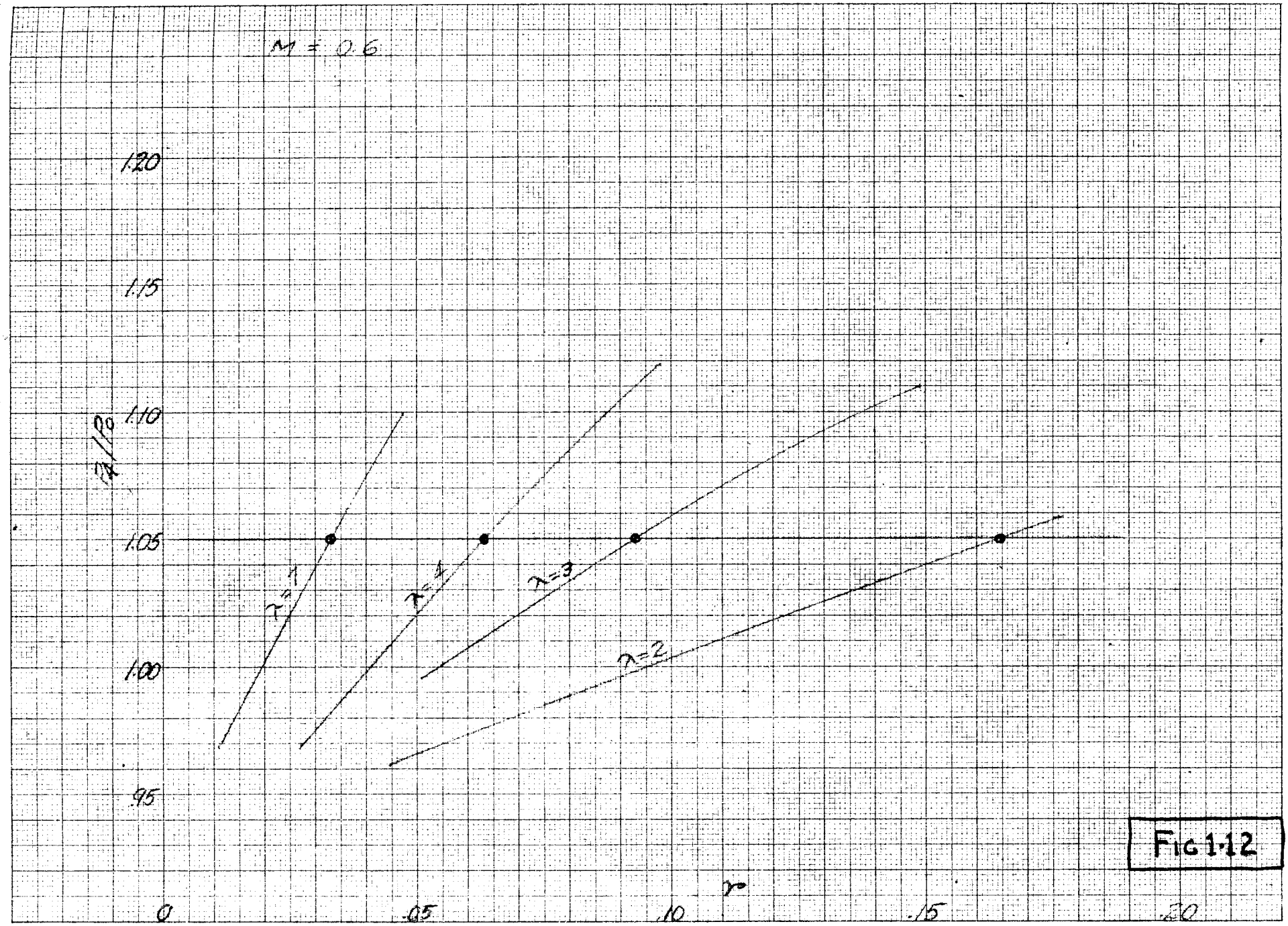

FIG 1-12

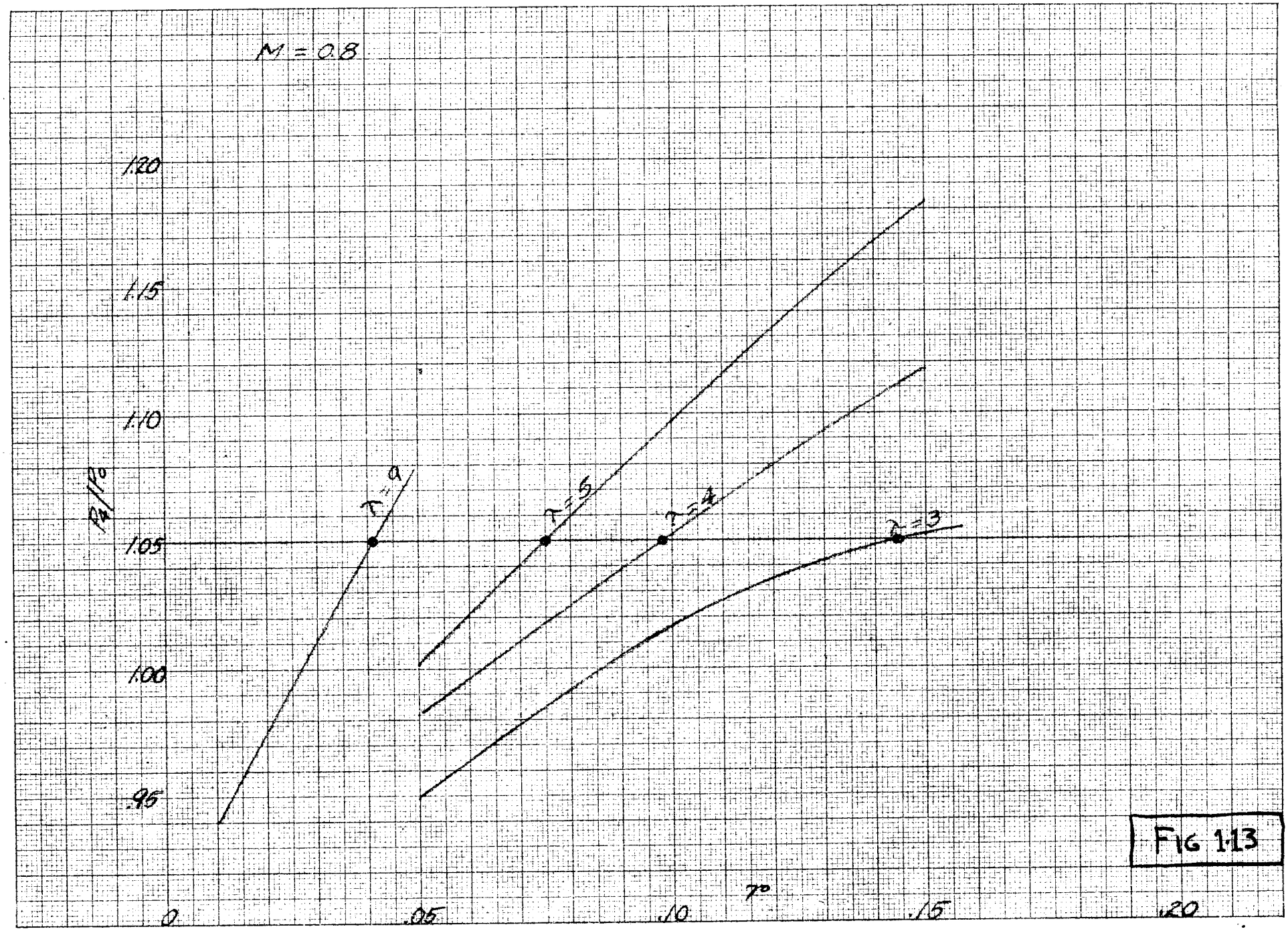
M = 0.8
1.20
1.15
1.10
1.05
1.00
.95
p_H/p_0
r = a
r = 5
r = 4
r = 3
0
.05
.10
.15
.20
θ°

Fig 1.13

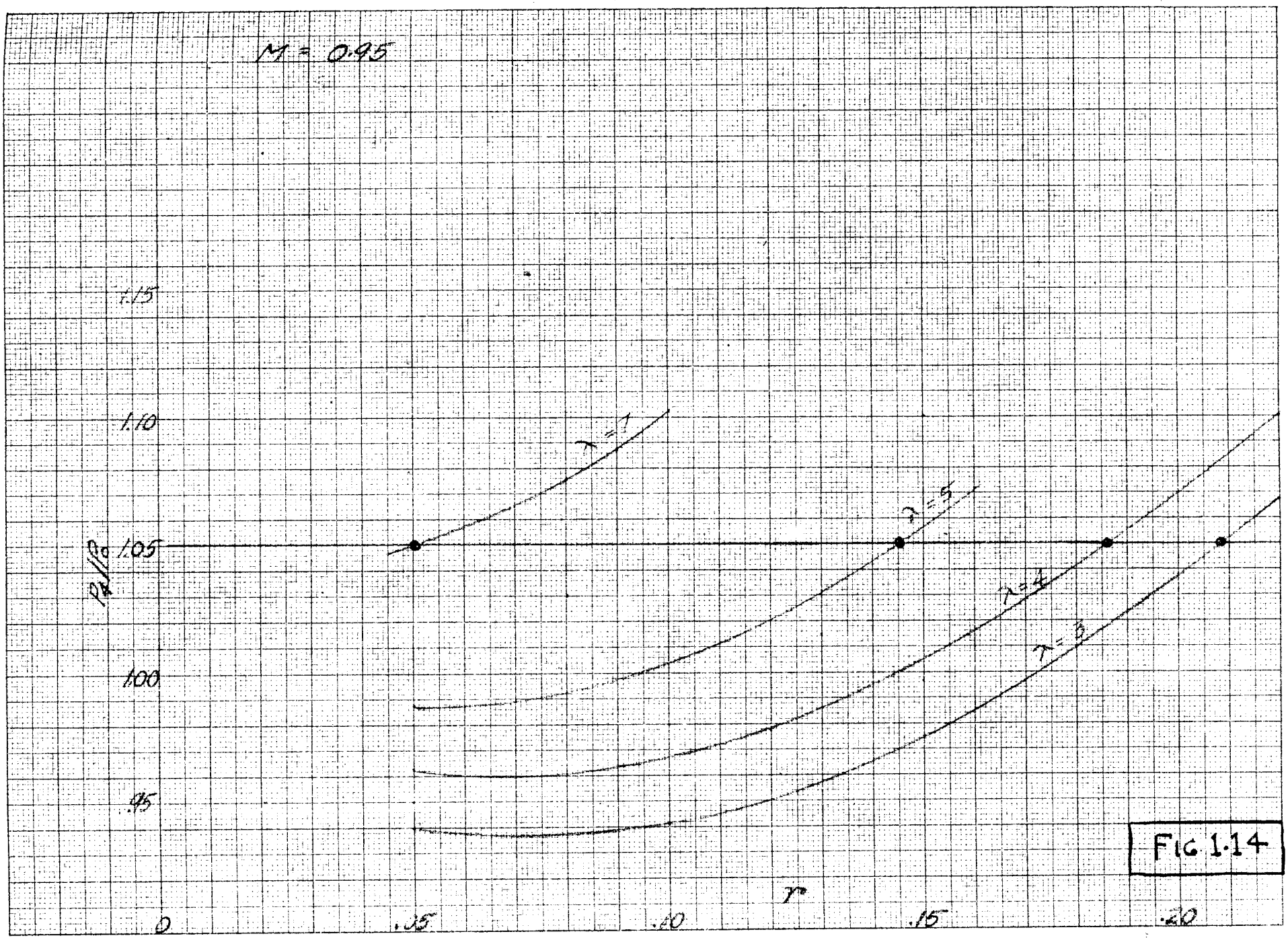

Fig 1.14

S E C T I O N 2

DESIGN

(A) Application of Theory

(B) Design Features

(A) Application of Theory

Theoretical Compressor Performance Based

on Constant Volumetric Efficiency

$$m = A_j \sqrt{\frac{2\gamma}{\gamma - 1} p_s \rho_s \left[\left(\frac{p}{p_s} \right)^{\frac{2}{\gamma}} - \left(\frac{p}{p_s} \right)^{\frac{\gamma+1}{\gamma}} \right]}$$

where m = mass flow = lbs. of air per second

A_j = Jet (Orifice) area

p_s, ρ_s = Supply (by compressor) pressure and density respectively

p = Pressure at jet ($\frac{p}{p_s}$ = 0.528 for air)

Assumptions:

Atmospheric pressure = po = 14.7 psi

Atmospheric temperature = $t_o = 70^oF$

Delivery air temperature = $t_s = 90^oF$

Delivery air humidity = 100%

The above equation reduces to:

(1) $$A_j = \frac{0.675\ m}{0.856}$$

where λ = compression ratio = $\frac{p_s}{p_o}$

Previous calibration of the compressors indicated that the delivery rate was approximately 2070 cfm for the parallel arrangement and 1670 cfm for the series arrangement. The mass rates of delivery were deduced from these volumetric rates and equation (1) was plotted, Fig. 2.1

The maximum compression ratios which could be expected were approximately 3.5 for the parallel arrangement and 6 for the series arrangement.

Entering Fig. 1.1 with these compression ratios, one can determine the ratio $\frac{\text{Jet Area}}{\text{working section area}}$ (A_j/A_3) for M = 1; from Fig. 2.1 , one can determine A_j for the same compression ratios; hence A_3 may be found.

λ	A_j/A_3 Fig. 1.1	A_j Fig. 2.1	A_3
3.5	.064	$2.7^{\text{"}2}$	$42.2^{\text{"}2}$
6	.022	$1.38^{\text{"}2}$	$62.6^{\text{"}2}$

Taking into consideration the theoretical nature of the compressor performance curves (Fig. 2.1) and knowing full well that a certain amount of leakage could be expected, the latter condition becoming increasingly serious at higher compression ratios, a conservative value of A_3 equal to $30^{\text{"}2}$ was selected. This should permit easy operation of the compressors with a minimum of high pressure air leakage.

This conservatism proved to be about correct as can be seen from Fig. where actual test data is also plotted. These test data represent the optimum attained in regard to elimination of high pressure air leakage.

Repeating the above analysis based on actual test data, we obtain:

λ	A_j/A_3 (Theor.)	A_j (Actual)	A_3
3.5	.064	$2.25^{\text{"}2}$	$35.2^{\text{"}2}$
6.0	.022	$0.54^{\text{"}2}$	$24.5^{\text{"}2}$

From the above it can be seem that the combination of reduced volumetric efficiency and increased high pressure at high compression ratios was so great that M = 1 could not be attainable in series operation for an $A_3 = 30^{\text{"}2}$, but would be attainable in parallel operation.

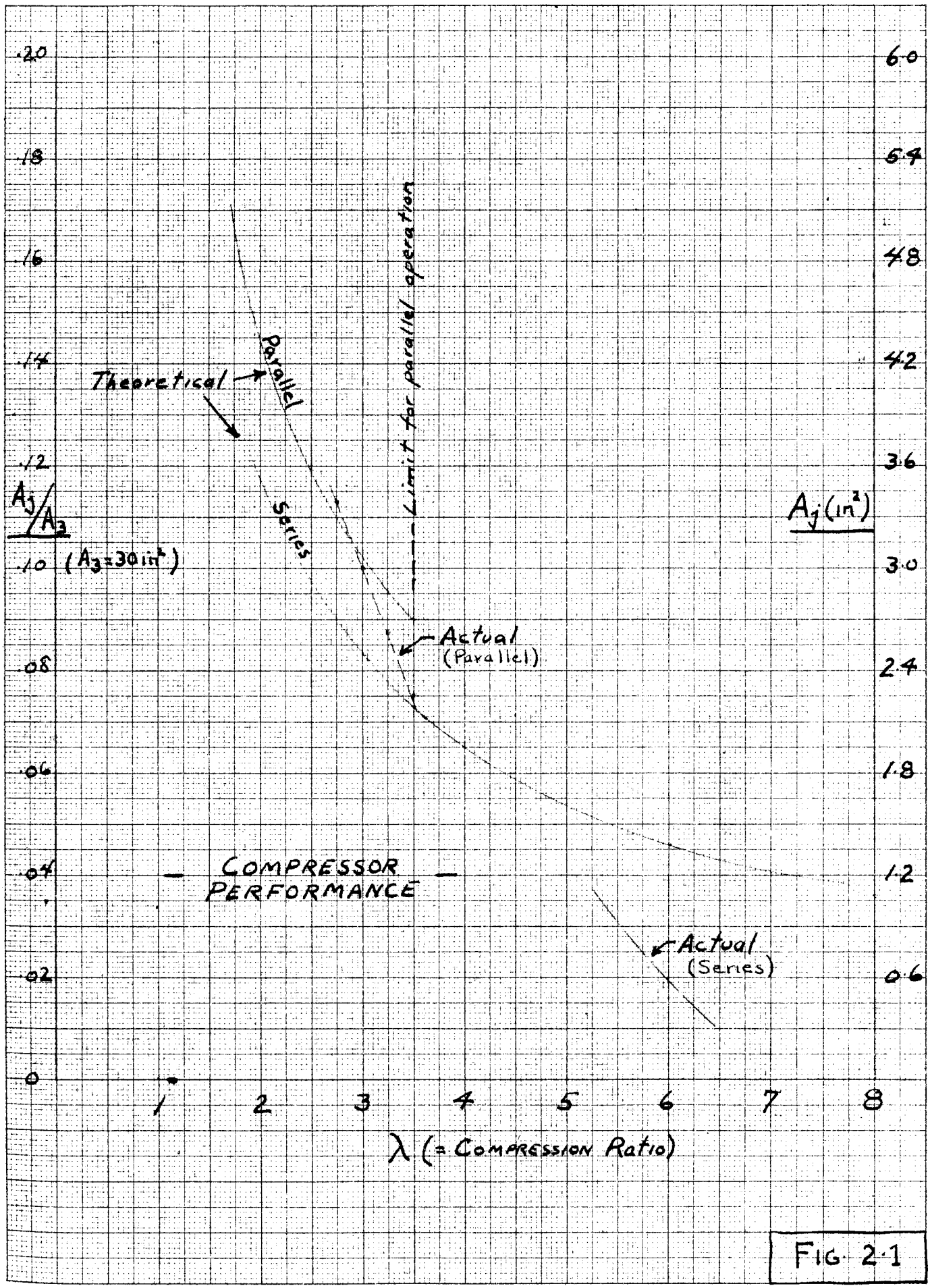
.20
.18
.16
.14
.12
.10
.08
.06
.04
.02
0
A_j/A_3
(A_3=30 in²)
6.0
5.4
4.8
4.2
3.6
3.0
2.4
1.8
1.2
0.6
A_j (in²)
Theoretical
Parallel
Series
Limit for parallel operation
Actual (Parallel)
Actual (Series)
COMPRESSOR PERFORMANCE
1
2
3
4
5
6
7
8
λ (= Compression Ratio)

FIG. 2-1

(B) DESIGN FEATURES

The general layout of the tunnel is shown in Dwg No. 00 (APPENDIX)

Dimensions:

Overall Length	36'	
Entrance Section Length	6'	
Contraction Section Length	2.75'	
Working Section Length	39.5"	
Mixing Section Length	10"	
Diffuser Length	19.3'	
Entrance Section Area	3' x 3 1/2'	= 10.5 sq. ft
Working Section Area	12" x 2.5"	= 30 sq. in. = 0.208 sq.ft.
Contraction Ratio	10.5/.208	= 50.5
Diffuser Exit Area	4' x 3'	= 12 sq. ft.

Mixing Section Area:

Minimum	- 12" x 2.5"	= 30 sq. in.	= 0.208 sq. ft.
Maximun	- 12" x 3"	= 36 sq. in.	= 0.250 sq. ft.

Divergence Angle of Diffuser:

Horizontal	— 6.0° (included angle)
Vertical	— 6.5° (included angle)

Air Supply:

Furnished by two (2) rotary compressors driven by a 200 hp. induction motor. The compressors may be connected in parallel or series, the former arrangement giving approximately 2100 cfm up to a maximum compression ratio of 3.5 while the latter gives approximately 1700 cfm up to a maximum compression ratio of 6.

Flexible Walls and Retaining Blocks:

See Photographs No. 1, 2, 3.

The material used for the flexible surface is .015" phosphor bronze sheet necessarily cut to close tolerances in width. The upstream end is secured by means of screws to the steel block, countersinking the phosphor bronze, filling with solder and filing down to give a smooth surface. The downstream end is free to slide underneath a short strip of phosphor bronze fastened to block by means of screws.

Each adjusting screw has 1" range, permitting 1/2" convergence of tunnel and 1/2" divergence. Thus, the working section may contain a throat 11" in height and the widest portion may be 13" in height. Each adjusting screw is provided with a gland and packing material to prevent leaks into working section. Each of the static pressure connections projecting from block are short brass ferrules, press fitted in holes bored to close tolerances.

The slots in the side faces of the retaining blocks are for purposes of sealing. Rubber strip is inserted and the pressure exerted by closing the windows creates a very effective seal.

Twenty-six (26) static connections are made along the centerline of the flexible wall, rubber tubing serving as flexible connectors from wall to block.

Speed Control:

Three methods are available for control of speed of induced flow in working section. One is merely a throttle valve on the compressor intake while the other two are distinctive design features of the tunnel.

One method employs the principle of creating a throat downstream of working section and just ahead of jets. This is accomplished by means of a pair of plates (see photographs No. 4 and No. 5) which form a part of the vertical walls of the tunnel. The surface of the plates is .015" phosphor bronze sheet and a means is provided for varying the shape of this surface from planar to a smooth convex profile projecting about 0.5" maximum into the induced airstream. This variation may be made while the tunnel is operating. If the tunnel speeds are sufficiently high to be able to produce a Mach No. = 1 in this throat, then any disturbances in the mixing section are prevented from disturbing the flow upstream in the working section.

The other method of speed control lies in the incorporation of variable sized jets described in the following section.

Variable Jets and Mixing Chamber:

See Dwg. No. 3-1

It will be noted that the above mentioned adjustable throat plates form one side of the jet, the fixed side. The other side of the jet is an integral portion of the mixing chamber vertical walls. The flexibility of these vertical walls permits variation of the jet size. This is accomplished by means of a screw and nut arrangement, the shaft of the screw passing thru the casting wall to the exterior where gears and shafting are employed to join both jets so that they may be varied simultaneously. The jet size may be varied while the tunnel is operating.

The mixing chamber walls may be adjusted so that the width of the chamber can be varied from approximately 2.75" to 3.00"; however, the construc-

Variable Jets and Mixing Chamber (con't):

tion is such that at the downstream end of mixing chamber (at the diffuser connection), the width is always 3.00".

Air Sealing Technique:

Rubber (sheet and tube) together with rubber cement was relied upon completely to solve the inevitable problem of sealing against both high and low pressure leaks.

In general the method consists of cementing the rubber over the leak (usually the very small gap between two carefully machined surfaces) and depending on the pressure itself to maintain the seal, the cement merely serving to hold the seal in place.

In the case of a leak at the junction of two pieces which can move relative to each other (e.g., the mixing chamber walls), a groove is cut in one surface and a 3/32" diameter rubber tube cemented in the groove. The air pressure serves to force the tube out of its original circular cross sectional shape and to effectively seal the joint as indicated in the sketch below:

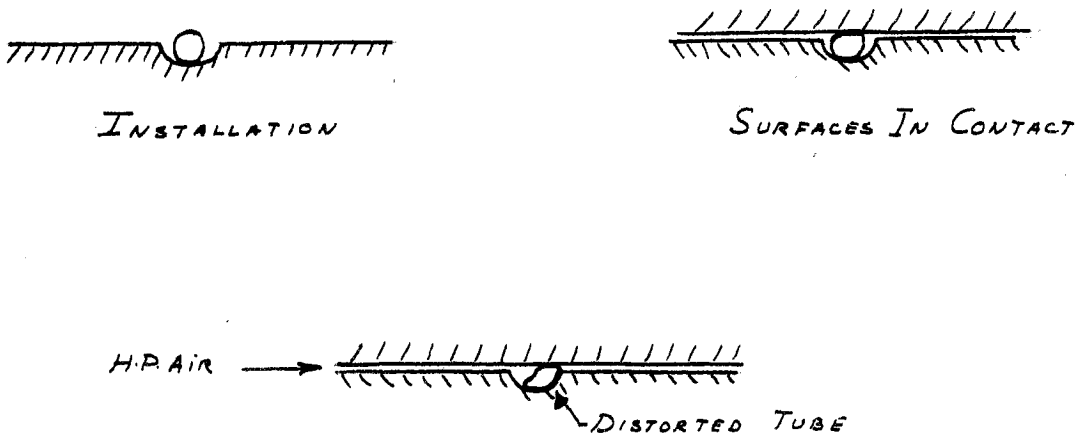

Air Sealing Technique: (cont)

Photograph No. 6 is a closeup of a window end sealing device (Photos No. 2 and 3 show this piece in place) showing the method of sealing employed. The beveled 1/8" rubber strip is forced against the window end surface by means of a pair of wedges actuated by a screw. The gap left by the wedging action is sealed by means of a thin rubber sheet cemented to the top and bottom pieces; a backing steel strip, secured to the longer piece by means of flush screws, resists the force of the air pressure and prevents the rubber sheet bulging into working section.

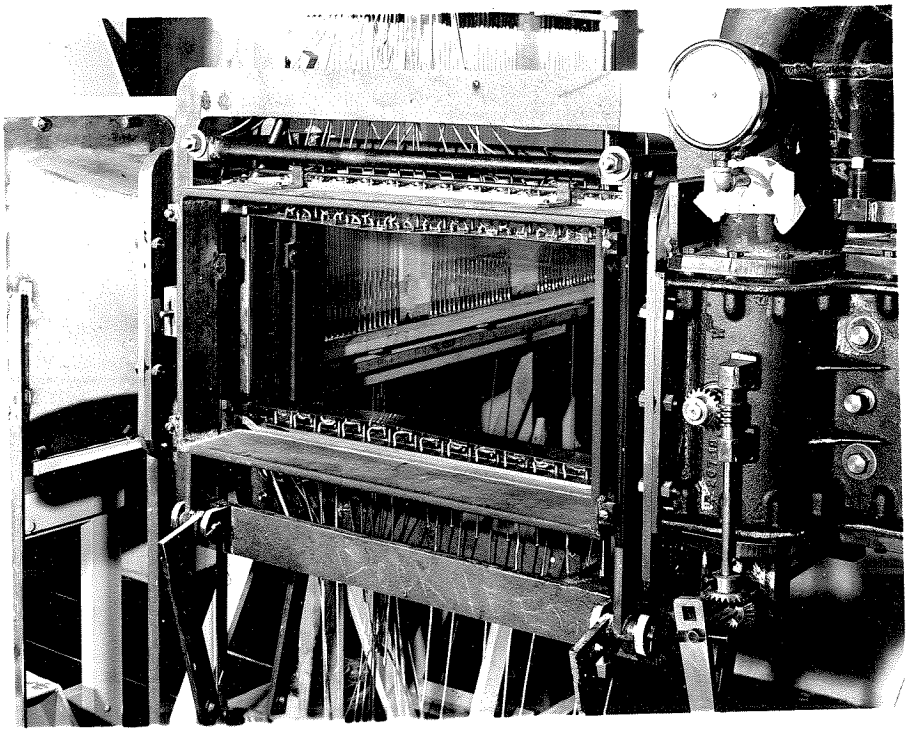

#1

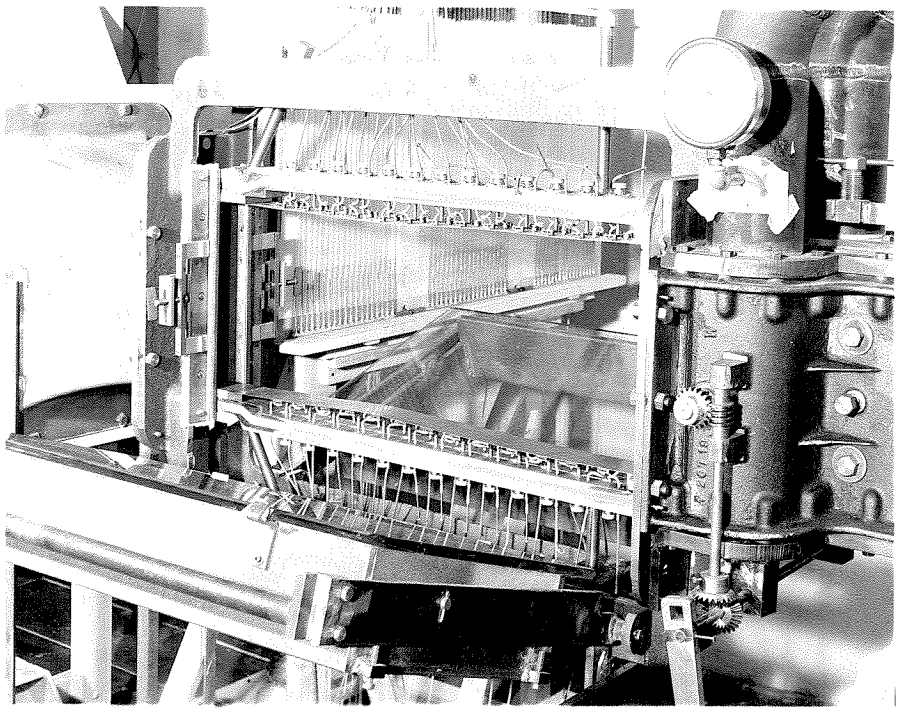

#2

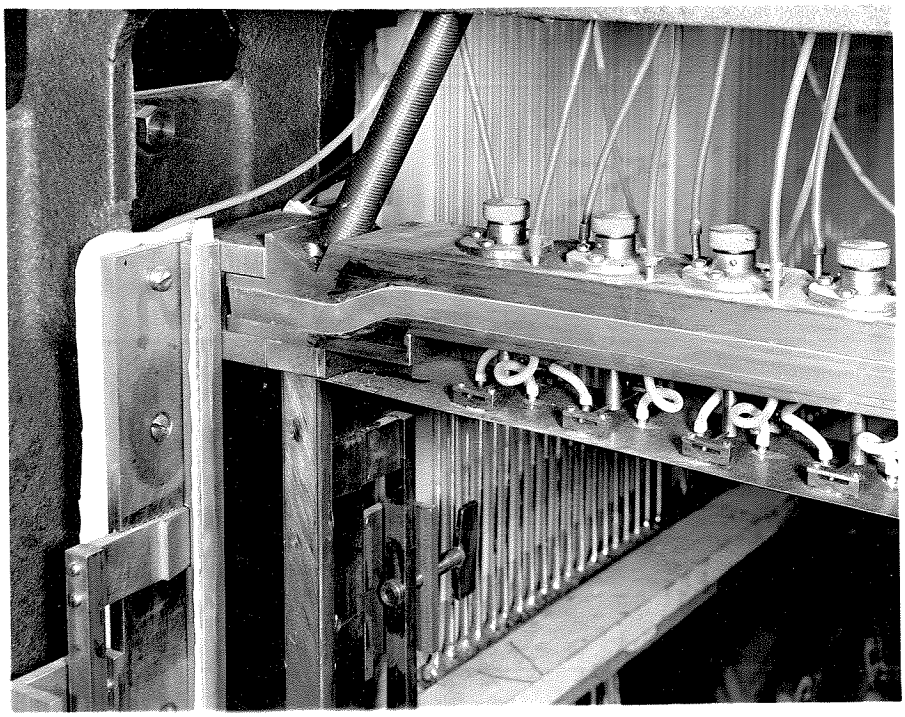

#3

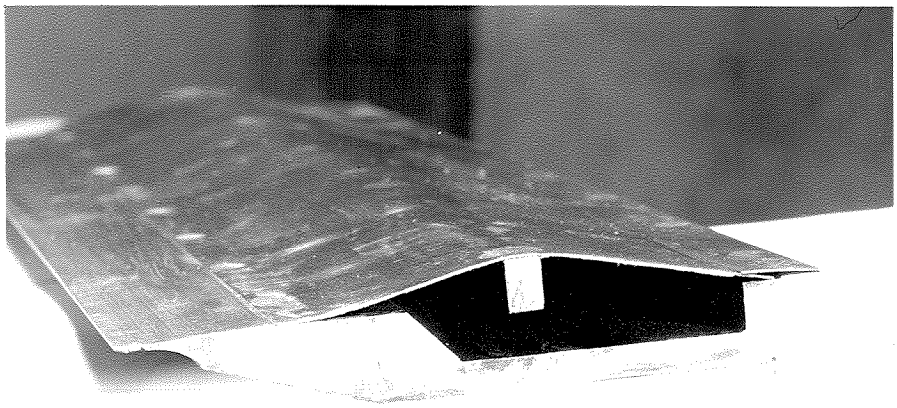

#4

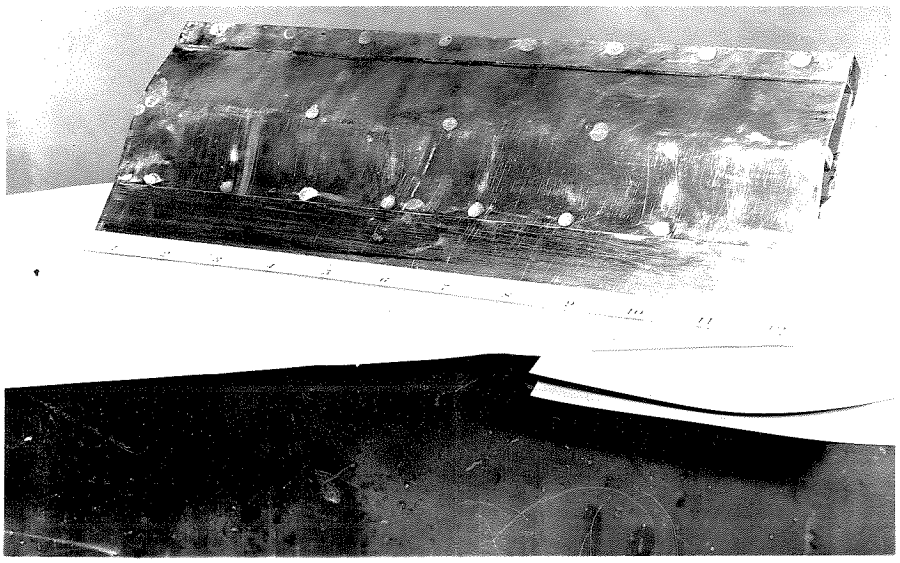

#5

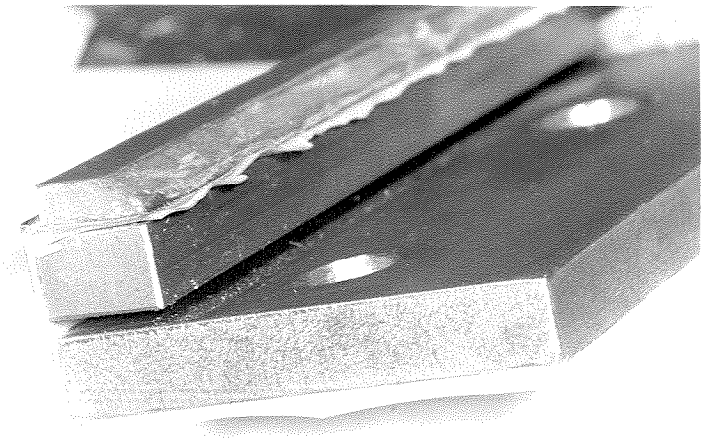

#6

S E C T I O N 3

PERFORMANCE

(A) Tunnel Performance

(B) Analysis and Discussion

(A) TUNNEL PERFORMANCE

(1) Optimum Performance Obtained:

The maximum Mach number attainable was found to be 0.655 with tunnel walls set parallel throughout. On page 3.4 is given a Table of Detailed Performance Data for a range of operating conditions; plots of these data superimposed on the theoretical performance curves may be seen by referring to Fig. 3.1 and Fig. 3.2. These data represent the optimum performance of the tunnel, i.e., leaks had been suppressed to a minimum, the modified jet plate was used, and the mixing section cross-sectional area was a maximum.

(2) Flow Conditions in Working Section:

No velocity surveys were made in working section but visual evidence seemed to indicate a turbulence free flow with a negligible boundary layer. With tunnel walls set parallel throughout, a loss of static head of 1 cm Hg. was recorded between the entrance and exit of working section. This figure compares very favorably with British data which specified a loss of 1" Hg. for a 2 1/4" circular tunnel whose working section length was of the order of 3-4".

(3) Adjustments Made to Attain Higher Mach Numbers:

(a) The shape of the jet was altered as indicated on Dwg. No. 3.1. It was thought that the direction of the air issuing from the original jet was inclined too much toward the induced air streams and a more efficient design would be to direct the jet approximately parallel to the induced flow; it was also believed that there was a slight choking effect in the mixing section and mutual jet interference effects because of this inclination. Hence, the jet was altered and the effect on performance was negligible but could be considered favorable.

(b) In the early stages of the operation of the tunnel, the adjustable walls in the mixing section were retracted as far as possible to

give a maximum mixing section area. The effect of this adjustment was to definitely improve the performance.

(c) In order to make the mixing area relatively larger, tests were made with vari-sized throats at various positions along working section; in addition, various positions of the vertical adjustable throat (just ahead of jets) were tested but in no case was any increase noted in the value of M attained except at the throat positions in the working section.

(d) Higher Mach numbers may be obtained for short periods of several seconds by means of "blow down" operation; i.e., the reservoir tank is pumped up to relatively high pressures and with compressors running, it is allowed to discharge through jets. With this type of operation, a Mach number of 0.8 is easily attainable.

(4) Diffuser Performance:

The nature of the flow issuing from the diffuser exit was very unsatisfactory; that is, the flow was quite irregular (puffy) over the exit area and, in the upper 6"-7" of the diffuser exit, a distinctly defined area of separation existed. Removal of the wooden portinn of the diffuser revealed this same region of separation at the exit of the metal diffuser. It is believed that this separation is due to a high pressure leak into the after upper portion of the working section at the joint between the working section and mixing section. The walls of the wooden diffuser eventually loosened up due to the vibration associated with the irregular diffuser flow.

(5) Jet Survey:

The construction of the high pressure chest in the mixing section casting is such that there appeared to be some question as to the constancy of flow over the entire length of the jet. A rough total head survey of both jets was made and the maximum variation of total head was

found to be 5 cm Hg. Contrary to what was anticipated, the maximum total head readings occurred at the top and bottom of the jet.

PERFORMANCE DATA

NOTE: All Pressures are in cm. Hg. unless otherwise noted

ASSUMED
p_o= 14.7psi
T_o= 75°F

Run No.	A_j/A_3	p_s (psi)	λ	Intake ("Hg Suction)	p_1	p_2	p_3	p_4	p_{ref}	M_2	M_3
		26.4	2.79	0.25	27.4	29.5	28.0	21.1	9.1	.6815	.655
		25.4	2.73	1.75	26.3	28.4	27.2	20.6	9.2	.66	.638
		20.5	2.37	5.5	23.5	24.4	23.5	18.6	9.25	.58	.56
30	.1125	16.5	2.12	8.0	20.7	21.7	21.0	16.9	9.30	.52	.50
(Parallel)		14.0	1.95	10.0	18.8	19.4	19.0	15.8	9.4	.46	.45
		11.75	1.80	12.0	17.5	18.0	17.5	14.8	9.5	.42	.405
		30.3	3.06	.25	27.1	29.1	27.6	21.8	9.1	.68	.65
		29.2	2.99	1.5	26.3	28.0	27.0	20.5	9.1	.655	.635
		24.0	2.63	5.0	24.1	25.5	24.5	18.8	9.2	.60	.58
31	.100	19.0	2.29	9.0	20.8	21.8	21.2	17.0	9.4	.52	.50
(Parallel)		11.8	1.80	14.0	16.3	16.7	16.4	13.9	9.5	.38	.375
		33.	3.26	1.5	26.2	28.0	26.8	20.8	9.15	.655	.63
32	.0875	28.	2.91	5.0	24.5	26.0	25.0	18.7	9.20	.61	.59
(Parallel)		19.	2.33	10.4	19.5	20.4	19.9	16.1	9.4	.485	.47
		37.2	3.53	1.5	26.9	29.	27.7	20.2	9.0	.68	.652
		36	3.85	1.5	26.2	28.2	27.1	19.9	9.1	.66	.637
		31.4	3.14	5.0	23.5	24.8	24.0	17.8	9.25	.58	.57
33	.075	27.8	2.89	8.0	22.	23.0	22.3	17.0	9.3	.545	.53
(Parallel)		23.0	2.56	11.0	19.	20.8	19.3	15.3	9.4	.495	.455
		76	6.16	1.		17.1		10.8	4.5	.52	.50)
		74	6.03	1.		15.5		10.2	4.5	.885	.87 }
		72	5.90	3.		15.0		9.7	4.7	.87	.86)
		65.6	5.86	8.		12.0		7.7	5.0	.375	.365)Est.
42	.0156	53.8	4.66	15.		9.0		6.7	5.0	.280	.27)
(Series)1		40.0	3.72	22.		7.1		6.0	5.0	.205	.195)

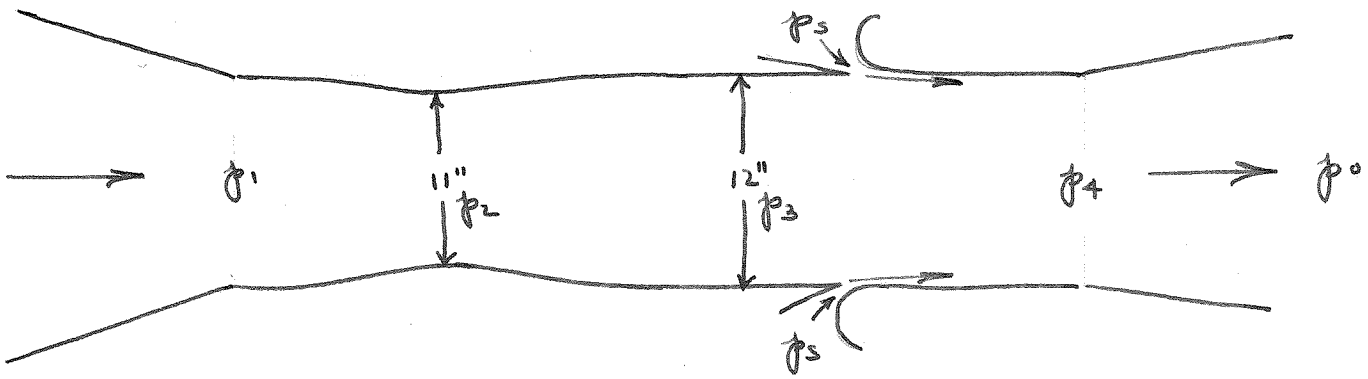

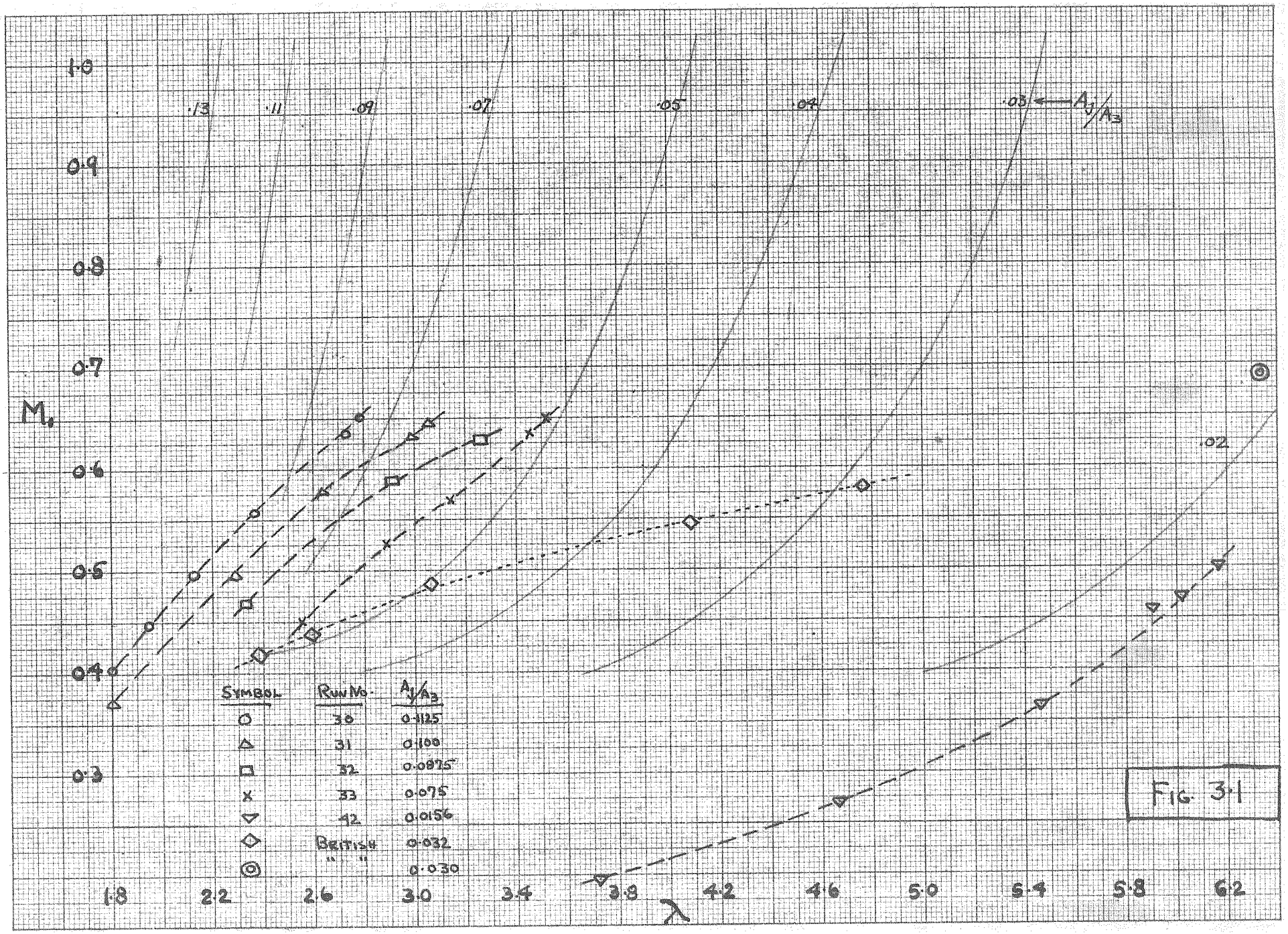
1·0
0·9
0·8
0·7
0·6
0·5
0·4
0·3
M₁
·13
·11
·09
·07
·05
·04
·03
A₁/A₃
·02
1·8
2·2
2·6
3·0
3·4
3·8
4·2
4·6
5·0
5·4
5·8
6·2
λ
SYMBOL
RUN No.
A₁/A₃
30 0·1125
31 0·100
32 0·0875
33 0·075
42 0·0156
BRITISH 0·032
" " 0·030

Fig. 3·1

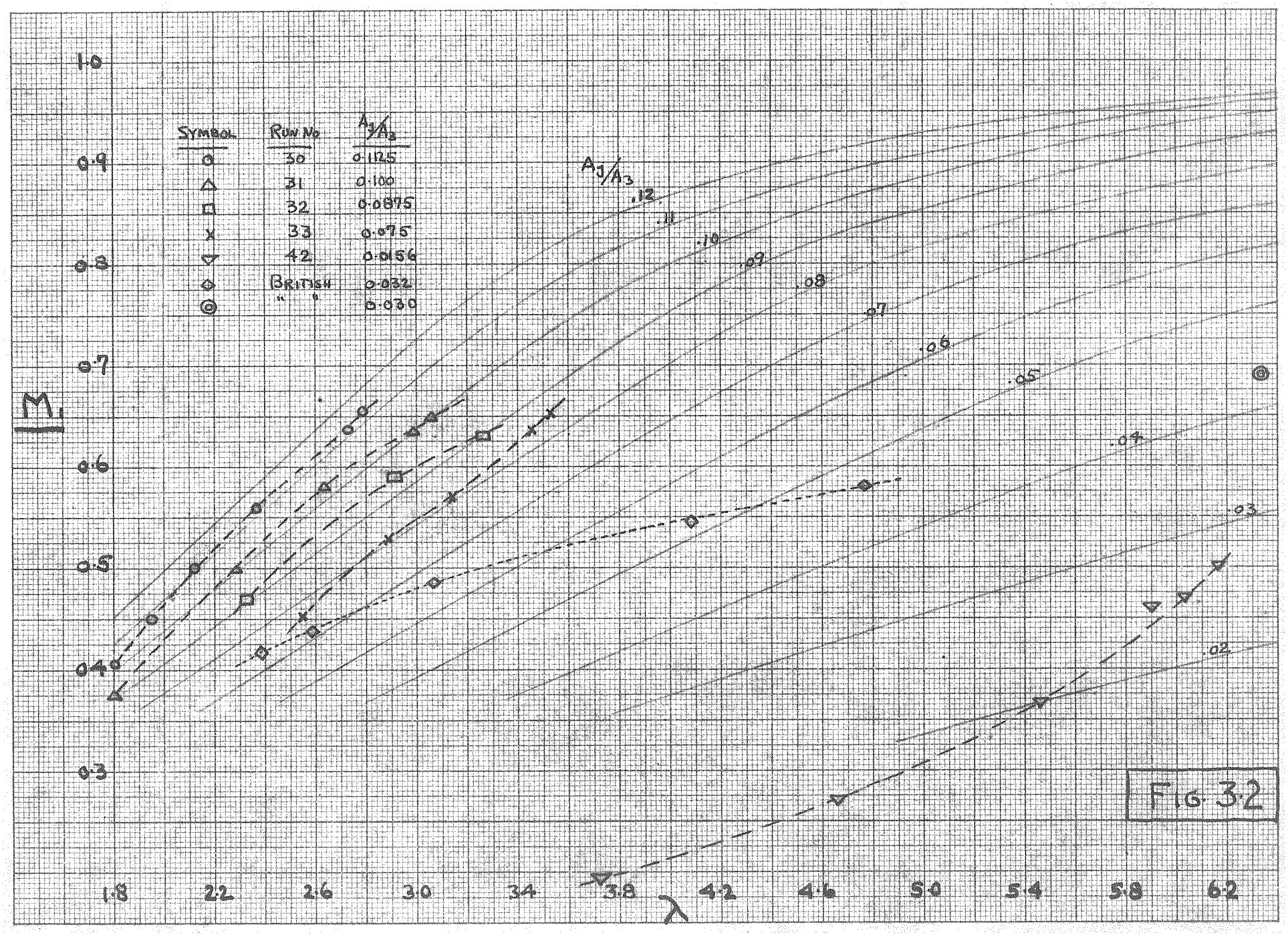
Symbol
Run No
A_1/A_2
○ 30 0.1125
△ 31 0.100
□ 32 0.0875
× 33 0.075
▽ 42 0.0156
◇ British 0.032
◎ " " 0.030
A_1/A_3
.12
.11
.10
.09
.08
.07
.06
.05
.04
.03
.02
M
1.0
0.9
0.8
0.7
0.6
0.5
0.4
0.3
1.8
2.2
2.6
3.0
3.4
3.8
4.2
4.6
5.0
5.4
5.8
6.2
λ

Fig. 3.2

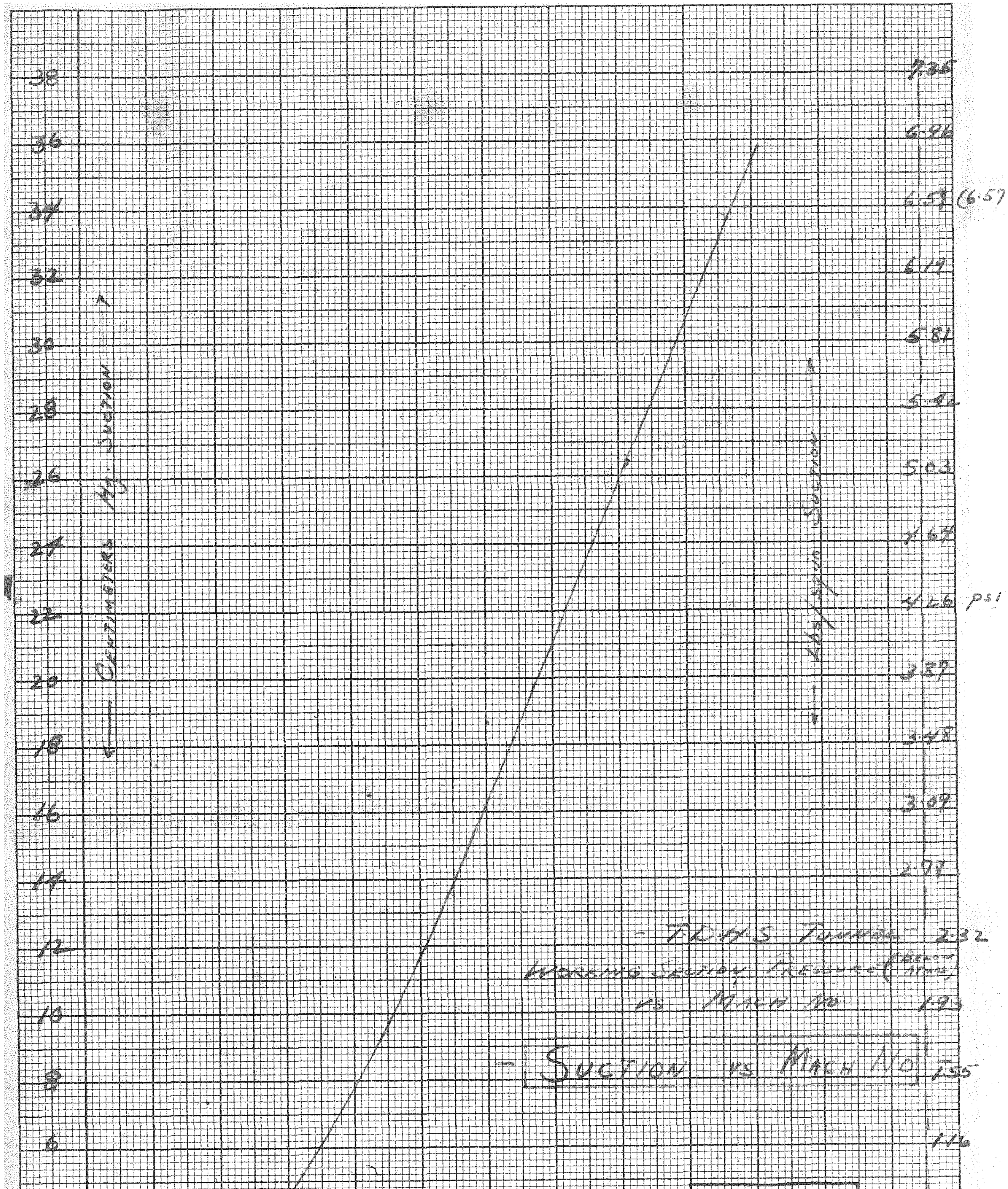
T.D.H.S. Tunnel
Working Section Pressure (Below Atms)
vs Mach No
Suction vs Mach No
Centimeters Hg Suction
Lbs/sq in Suction
psi
(6.57)
M₁
0
·1
·2
·3
·4
·5
·6
·7
·8
·9
1·0
0
2
4
6
8
10
12
14
16
18
20
22
24
26
28
30
32
34
36
38
0.39
0.77
1.16
1.55
1.93
2.32
2.71
3.09
3.48
3.87
4.26
4.64
5.03
5.42
5.81
6.19
6.57
6.96
7.35
RFK 4/3/43
Fig. 3.3

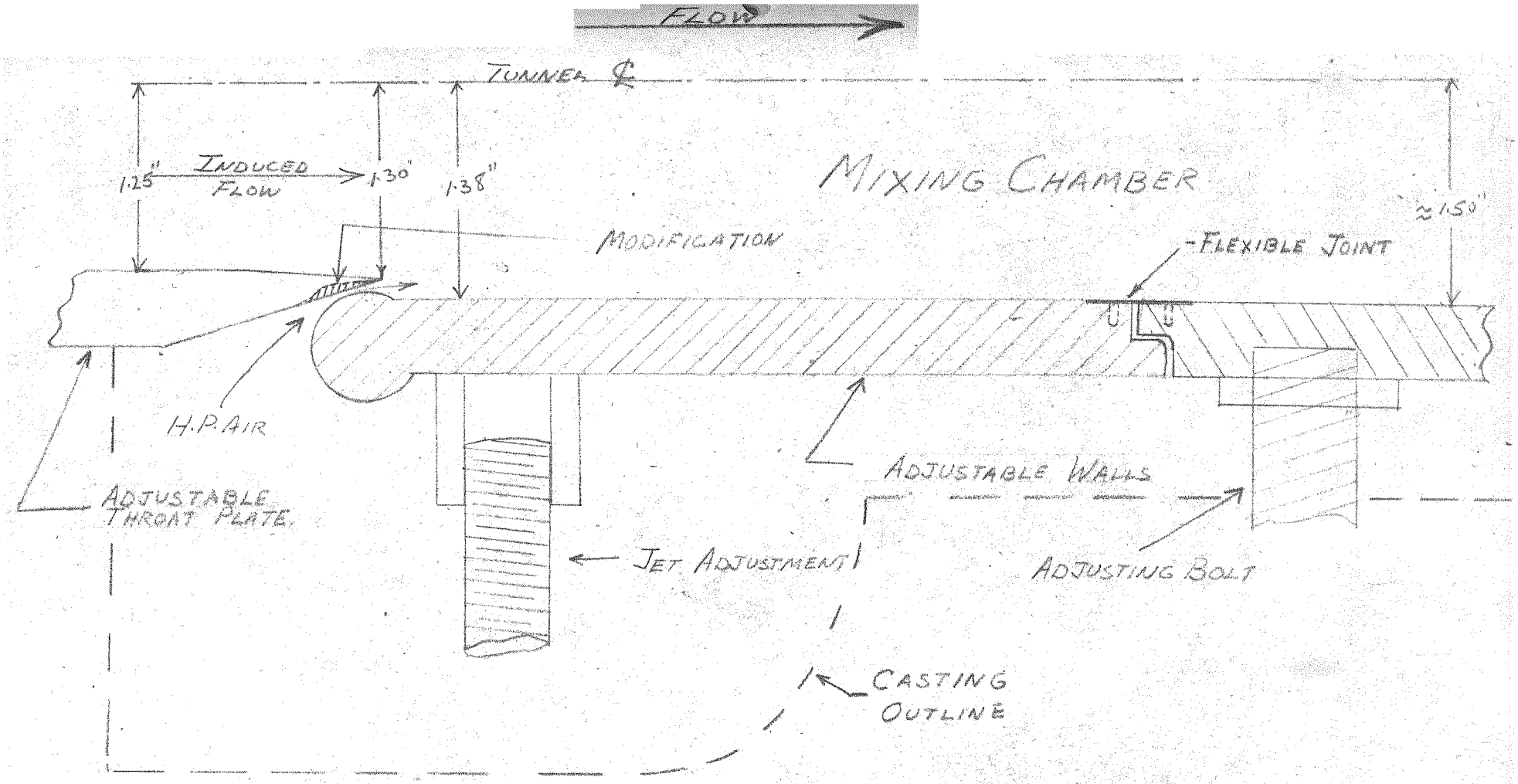

							TOLERANCES ± .010 OR 1/64 UNLESS OTHERWISE NOTED
MATERIAL	FINISH	HEAT TREAT	DRAFTSMAN	CHECKED	APPROVED	ENGINEER	
GUGGENHEIM AERONAUTICAL LABORATORY CALIFORNIA INSTITUTE OF TECHNOLOGY			JET + MIXING CHAMBER - ORIGINAL + MODIFICATION -				# 3-1
			NAME				DRAWING NO.

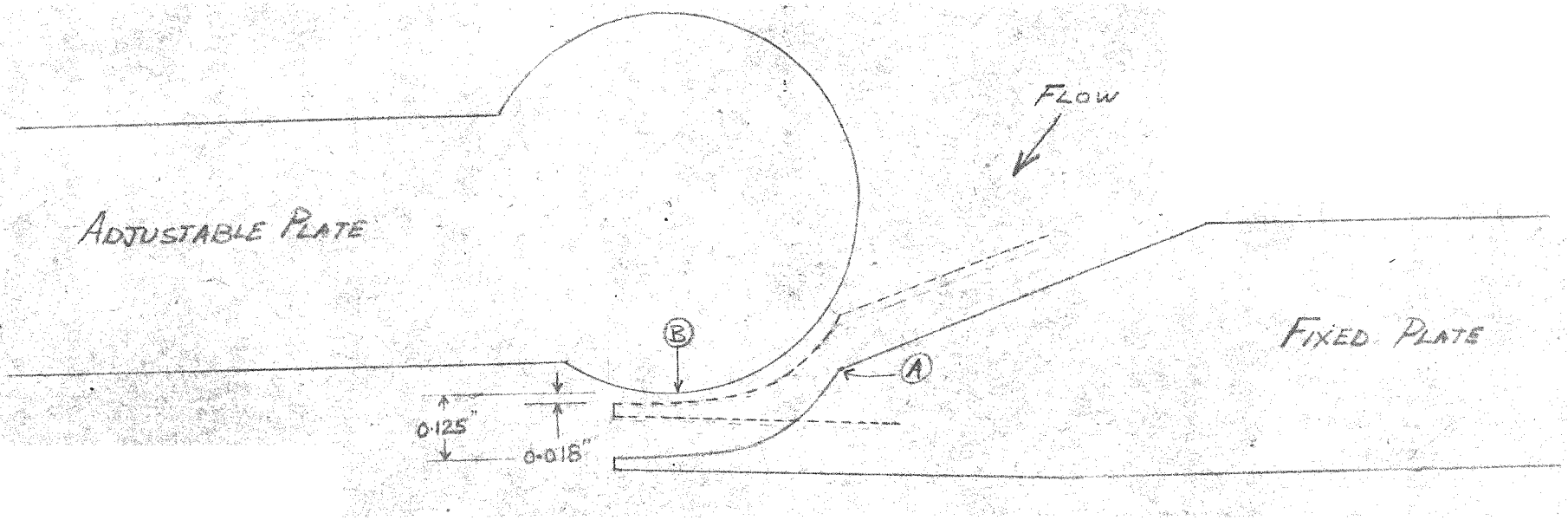

							TOLERANCES ± .010 OR 1/64 UNLESS OTHERWISE NOTED
MATERIAL	FINISH	HEAT TREAT	DRAFTSMAN	CHECKED	APPROVED	ENGINEER	SCALE 3/1
GUGGENHEIM AERONAUTICAL LABORATORY CALIFORNIA INSTITUTE OF TECHNOLOGY			ACTUAL JET SHAPE and DIMENSIONS FOR EXTREME JET OPENINGS				#3-2
			NAME				DRAWING NO.

(B) ANALYSIS AND DISCUSSION

(1) Referring to Fig. 3.1 and 3.2, two facts stand out:

First, the calibration runs with the compressors in parallel (Runs No. 30, 31, 32 and 33) do not have any of the characteristics predicted by the theoretical performance curves for the Supersonic Jet Theory, but they do fit remarkably well into the theoretical curves predicted by the Sonic Jet Theory.

Secondly, the calibration run (No. 42) with the compressors in series has the opposite tendency; that is, it fits the Supersonic Theory rather well and definitely does not fit the Sonic Jet Theory.

From these facts it may be inferred that the tunnel operates on the Sonic Jet Theory at low compression ratios (large jet openings) and on the Supersonic Jet Theory at high compression ratios (small jet openings).

It will be noted that, although run No. 42 depicts the tunnel operating as designed (on the Supersonic Jet Theory), a higher Mach number was not obtained because of the relatively larger amount of high pressure leakage experienced at these high compression ratios, plus the effect of reduced compressor volumetric efficiency near the end of its range of operation. (See Fig. 2.1)

(2) One possible explanation of the contradictory performance of the tunnel as described in (1) above is that, at large jet openings, the supersonic expansion of the jet is practically nil, thereby producing exit velocities very close to the speed of sound, and, at small jet openings, the supersonic expansion is about correct and therefore the

Supersonic Jet performance is closely paralleled.

Accordingly, the relative positions of the two plates which form the jet were obtained by means of a wax impression; then both plates were removed and pertinent measurements of each taken by means of a dial micrometer gauge.

It may be seen (Dwg. No. 3.2) that for large jet openings, the throat of the jet is located at "A", while for small jet openings, the throat occurs further downstream at point "B". For intermediate jet openings approximately equal throats occur at points "A" and "B".

The only jet opening at which the jet resembles a true supersonic nozzle is the small one. The shape of the nozzle at large jet openings is obviously far from a supersonic shape due to the discontinuity at "A", the very throat of the jet. At intermediate openings, the existence of two throats of approximately the same size is undoubtedly sufficient cause to make the jet depart radically from a supersonic nozzle. At small jet openings, there is no longer a throat at "A"; a gradual convergence takes place up to the throat at "B" and a smooth expansion follows.

(3) For the case of run No. 42 (A_j/A_3 = .0156) measurements of the throat and nozzle exit areas gave an expansion ratio of 1.74 which compares favorably with the calculated value of 1.58 (compression ratio = 6, M = 0.46). The actual expansion ratio is probably somewhat smaller than 1.74 because, referring to Fig. 3.1, it is seen that the parameter for run No. 42 should be an A_j/A_3 = 0.018 (approx) whereas it was recorded as 0.0156. This latter value could easily be in error by ±.0.005 (as could all A_j/A_3 values) because of the difficulty associated with determining exactly when the jets are closed. Thus, if A_j/A_3 = 0.018 for run No. 42 (instead of 0.0156) the actual expansion ration becomes 1.53

which agrees quite closely with the calculated value of 1.58.

(4) Referring to Fig. 3.2, a close comparison of the actual performance (Runs No. 30, 31, 32 and 33) with that predicted by the Sonic Jet Theory reveals that as the jet opening becomes smaller (A_j/A_3 decreases), the agreement between actual and theoretical values of the parameter (A_j/A_3) changes from very close agreement (Run No. 30) to a fair agreement (Run No. 33). For the smaller jet opening (Run No. 33) performance is definitely better than that predicted by theory, but is not better than that predicted by the Supersonic Jet Theory (Refer Fig. 3.1). This fact plus the additional observation that the shape of the performance curve for Run No. 33 (above a compression ratio of 3) indicates the characteristic shape predicted by the Supersonic Jet Theory lends support to the conclusion that the jet tends to assume a supersonic shape as the jet opening decreases.

(5) On Figs. 3.1 and 3.2 are plotted some data representing typical performance of British types of induction wind tunnels. For purposes of comparing performance on the same basis, the original British data had to be reduced to our performance parameters (See Appendix, Part C).

From Fig. 3.2 it may be seen that their performance is similar to that predicted by the Sonic Jet Theory. This agrees with their practice of using convergent nozzles (no supersonic expansion). However, their performance is definitely more efficient than ours to date; that is, for the same compression ratio, they obtain a higher Mach number with a smaller jet opening - which means a relatively smaller mass flow of motive air. Likewise, their actual performance is better than that predicted by the Supersonic Jet Theory for low compression ratios but

is not as good for high compression ratios. This would seem to indicate that the British practice of using an expanding mixing section is quite beneficial at low compression ratios only.

SECTION 4

CONCLUSION

(A) Conclusions

(B) Recommendations

(A) CONCLUSIONS

(1) In its present form, the tunnel performs in accordance with the Sonic Jet Theory at low compression ratios and in accordance with the Supersonic Jet Theory at high compression ratios.

(2) Mach numbers approaching unity were not attained at low compression ratios because of poor jet performance and, at high compression ratios, because of the large amount of high pressure leakage together with a reduced compressor output near the end of its operating range. The poor jet performance is explained by the inefficient jet shape at large jet openings.

(3) The Supersonic Jet Theory predicts a more efficient operation than the Sonic Jet Theory.

(4) The British design, i.e., a sonic jet plus an expanding mixing section, is more efficient than the Sonic Jet Constant Area Mixing design. In addition, the British design is more efficient than that predicted by the Supersonic Jet Theory at low compression ratios, but is less efficient at high compression ratios.

DESIGN CONDITION:
COMPRESSION RATIO - 3
JET THROAT - 0.125"
COMPRESSORS - PARALLEL
MACH NO. WORKING SECT = 1

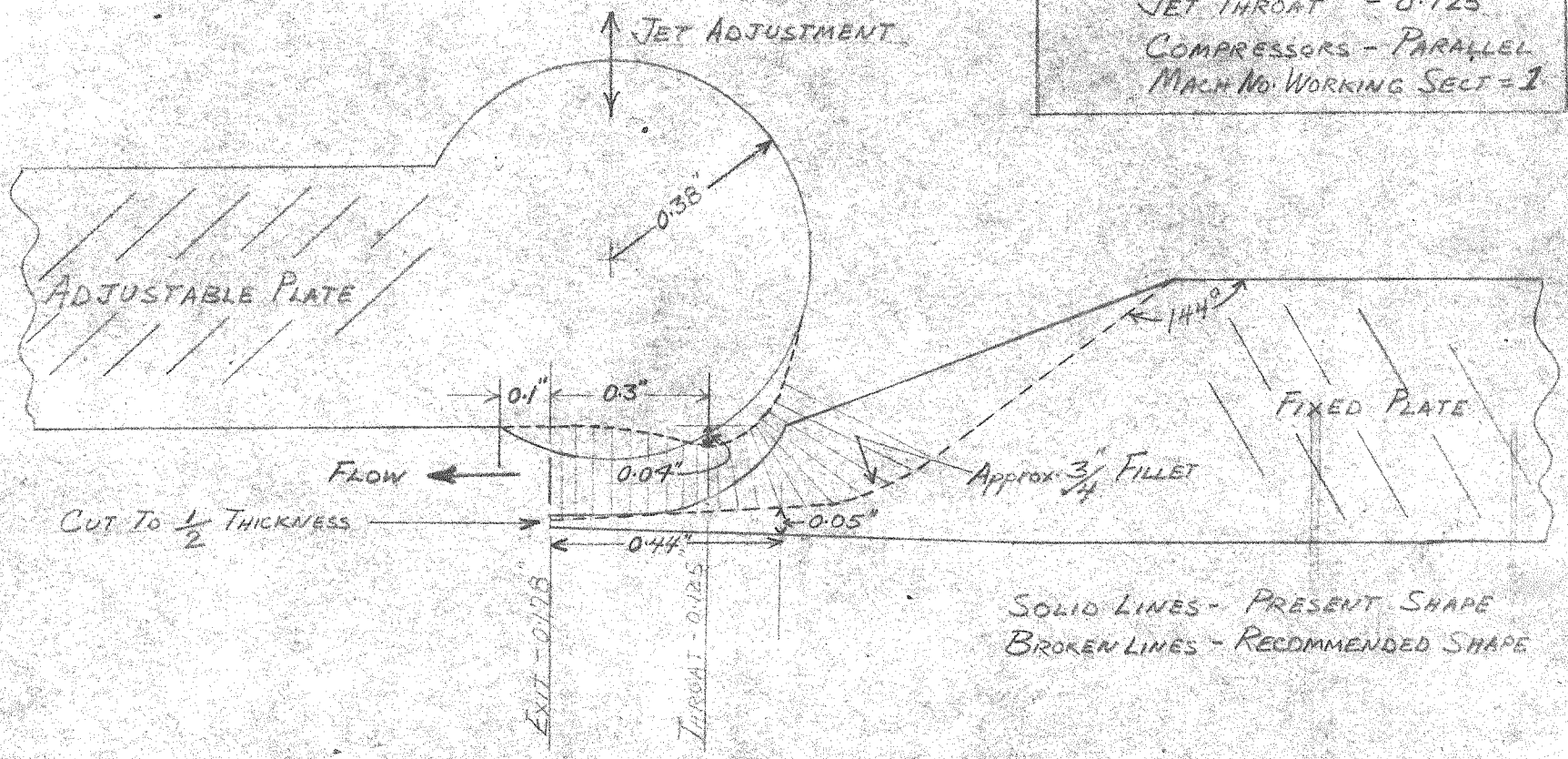

SOLID LINES - PRESENT SHAPE
BROKEN LINES - RECOMMENDED SHAPE

MATERIAL	FINISH	HEAT TREAT	DRAFTSMAN	CHECKED	APPROVED	ENGINEER	TOLERANCES ± .010 OR 1/64 UNLESS OTHERWISE NOTED
							SCALE 3/1

GUGGENHEIM AERONAUTICAL LABORATORY
CALIFORNIA INSTITUTE OF TECHNOLOGY

T.D.H.S. TUNNEL
RECOMMENDED JET MODIFICATION
NAME

#4.1
DRAWING NO.

(B) RECOMMENDATIONS

(1) A recommended modification of jets is shown in Dwg. No. 4.1. The recommended design condition of a compression ratio of 3 represents a compromise based on the following considerations:

(a) High pressure leakage: negligible at compression ratio of 3.

(b) Jet opening: Large - easier to machine accurately.

(c) Choking effect - operating at compression ratios lower than 3 (larger jet openings) is more likely to produce a throat in the mixing section.

(2) Eliminate high pressure leak in ceiling of working section at joint between working section casting and mixing section casting.

(3) Construct the necessary equipment and make a complete survey of the nozzle exits at various jet openings to determine the exit velocity.

(4) Modify mixing section so as to provide a greater degree of expansion. There is sufficient material in casting to increase exit of mixing section from 3" to 4"

(5) Brace the walls of the wooden diffuser more securely.

(6) A recommended extensive modification of the mixing section would include:

(a) Recommendation No. 4.

(b) Replacement of adjustable walls with integral walls. This would eliminate a serious source of high pressure leakage and, at the same time, would necessarily call for a non-variable jet. The latter change would be advantageous from the point of view of obtaining a jet of uniform throat size over its entire length. Speed control could be easily maintained by throttling the compressor intake or by means of a "Venetian blind" arrangement at diffuser exit.

SECTION 5

APPENDIX

(A) Supersonic Jet Theory Detailed Development and Calculations

(B) Sonic Jet Theory Calculations

(C) Reduction of British Data

(A) Super-sonic Jet Theory

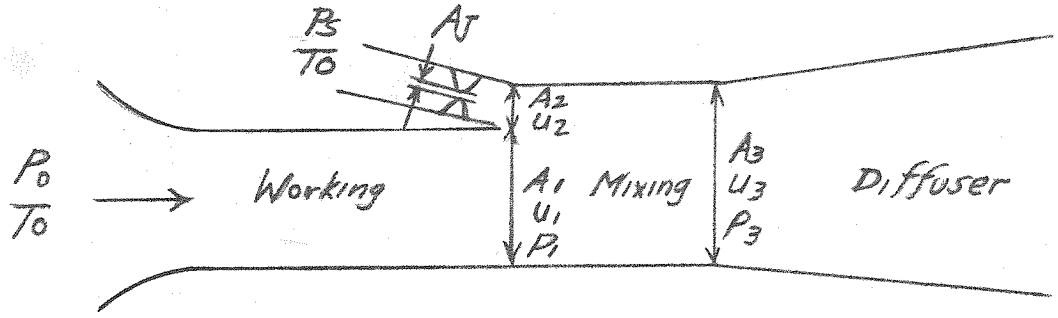

$$A_3 = A_1 + A_2 \;;\; A_2/A_3 \ll 1$$

The theoretical operations within the tunnel may be obtained from the following three equations:

Momentum;

$$① \quad A_3(p_1 - p_3) = A_3 \rho_3 u_3^2 - \{A_2 \rho_2 u_2^2 + A_1 \rho_1 u_1^2\}$$

Continuity;

$$② \quad A_3 u_3 \rho_3 = A_2 u_2 \rho_2 + A_1 u_1 \rho_1$$

$$m_3 = m_2 + m_1$$

Energy;

$$③ \quad \left(\frac{u_3^2}{2} + \frac{\gamma}{\gamma-1}\frac{p_3}{\rho_3}\right)\rho_3 u_3 A_3 =$$

$$\left(\frac{u_2^2}{2} + \frac{\gamma}{\gamma-1}\frac{p_2}{\rho_2}\right)\rho_2 u_2 A_2 + \left(\frac{u_1^2}{2} + \frac{\gamma}{\gamma-1}\frac{p_1}{\rho_1}\right)\rho_1 u_1 A_1$$

Since T is the same for both the induced and compressed air supply,

$$\frac{\gamma}{\gamma-1}\frac{p_1}{\rho_1} + \frac{u_1^2}{2} = \frac{\gamma}{\gamma-1}\frac{p_2}{\rho_2} + \frac{u_2^2}{2} \equiv \frac{C}{2}$$

④ $\therefore C = \frac{\gamma}{\gamma-1}\frac{p_3}{\rho_3} + \frac{u_3^2}{2}$

solving for p_3, u_3,

⑤ from ②, $\rho_3 = \frac{m_1 + m_2}{u_3 A_3}$

from ④, $\frac{\gamma}{\gamma-1}\frac{u_3 A_3 p_3}{m_1 + m_2} + \frac{u_3^2}{2} - C = 0$

$$u_3^2 + \frac{2\gamma}{\gamma-1}\cdot\frac{u_3 A_3 p_3}{m_1 + m_2} - 2C = 0$$

⑥ $$u_3 = -\frac{\gamma}{(\gamma-1)}\frac{A_3 p_3}{(m_1+m_2)} \pm \sqrt{\left(\frac{\gamma}{\gamma-1}\right)^2\left(\frac{A_3 p_3}{m_1+m_2}\right)^2 + 2C}$$

substituting ⑤ and ⑥ in ①,

$$p_1 - p_3 = \frac{m_1 + m_2}{A_3}u_3 - \frac{m_1 u_1 + m_2 u_2}{A_3}$$

$$p_1 - p_3 = \frac{m_1+m_2}{A_3}\left\{\frac{\gamma}{\gamma-1}\cdot\frac{p_3 A_3}{m_1+m_2} + \sqrt{\left(\frac{\gamma}{\gamma-1}\cdot\frac{p_3 A_3}{m_1+m_2}\right)^2 + 2C}\right.$$

$$\left. - \frac{m_1 u_1 + m_2 u_2}{A_3}\right\}$$

$$= -\frac{\gamma}{\gamma-1}p_3 + \sqrt{\left(\frac{\gamma}{\gamma-1}p_3\right)^2 + 2C\left(\frac{m_1+m_2}{A_3}\right)^2}$$

$$- \left(\frac{m_1 u_1 + m_2 u_2}{A_3}\right)$$

$$p_1 + \frac{p_3}{\gamma-1} + \frac{m_1 u_1 + m_2 u_2}{A_3} = \sqrt{\left(\frac{\gamma}{\gamma-1}p_3\right)^2 + 2C\left(\frac{m_1+m_2}{A_3}\right)^2}$$

$$\frac{p_3^2}{(\gamma-1)^2} + \frac{2p_3}{\gamma-1}\left[p_1 + \frac{m_1 u_1 + m_2 u_2}{A_3}\right] + \left[p_1 + \frac{m_1 u_1 + m_2 u_2}{A_3}\right]^2 =$$

$$\left(\frac{\gamma}{\gamma-1}p_3\right)^2 + 2C\left(\frac{m_1+m_2}{A_3}\right)^2$$

$$p_3^2\frac{\gamma^2-1}{(\gamma-1)^2} - p_3\frac{2}{\gamma-1}\left[p_1 + \frac{m_1 u_1 + m_2 u_2}{A_3}\right] - \left[p_1 + \frac{m_1 u_1 + m_2 u_2}{A_3}\right]^2 +$$

$$2C\left[\frac{m_1+m_2}{A_3}\right]^2 = 0$$

$$p_3^2 - p_3 \frac{2}{\gamma+1}\left[p_1 + \frac{m_1u_1 + m_2u_2}{A_3}\right] - \frac{\gamma-1}{\gamma+1}\left[p_1 + \frac{m_1u_1 + m_2u_2}{A_3}\right]^2 +$$

$$2C\frac{\gamma-1}{\gamma+1}\left[\frac{m_1 + m_2}{A_3}\right]^2 = 0$$

$$p_3 = \frac{1}{\gamma+1}\left[p_1 + \frac{m_1u_1 + m_2u_2}{A_3}\right] \pm$$

$$\sqrt{\left\{\frac{1}{\gamma+1}\left[p_1 + \frac{m_1u_1 + m_2u_2}{A_3}\right]\right\}^2 + \frac{\gamma-1}{\gamma+1}\left[p_1 + \frac{m_1u_1 + m_2u_2}{A_3}\right]^2 - 2C\frac{\gamma-1}{\gamma+1}\left[\frac{m_1+m_2}{A_3}\right]^2}$$

$$⑦\quad p_3 = \frac{1}{\gamma+1}\left[p_1 + \frac{m_1u_1 + m_2u_2}{A_3}\right] \pm \sqrt{\frac{\gamma^2}{(\gamma+1)^2}\left[p_1 + \frac{m_1u_1 + m_2u_2}{A_3}\right]^2 - 2C\frac{\gamma-1}{\gamma+1}\left[\frac{m_1+m_2}{A_3}\right]^2}$$

$$\dot{m}_1u_1 = A_1\rho_1u_1^2; \quad \frac{m_1u_1}{p_1} = \frac{A_1\rho_1u_1^2\gamma}{p_1\gamma} = \gamma A_1M_1^2$$

$$\frac{m_2u_2}{p_2} = \gamma A_2M_2^2$$

$$C = \frac{u_3^2}{2} + \frac{\gamma}{\gamma-1}\frac{p_3}{\rho_3} = \frac{\gamma}{\gamma-1}\frac{p_0}{\rho_0} = \frac{a_0^2}{\gamma-1} = \frac{\gamma+1}{2(\gamma-1)}a^{*2}$$

$$\frac{p_3}{p_1} = \frac{1}{\gamma+1}\left[1 + \frac{m_1 u_1}{p_1} + \frac{m_2 u_2}{p_2}\right]\frac{1}{A_3} \pm$$

$$\sqrt{\frac{\gamma^2}{(\gamma+1)^2}\left[\frac{p_1^2}{p_1^2} + \frac{2p_1}{A_3}\left\{\frac{m_1 u_1}{p_1} + \frac{m_2 u_2}{p_1}\right\} + \frac{m_1^2 u_1^2}{p_1^2} + \frac{2 m_1 u_1}{p_1}\cdot\frac{m_2 u_2}{p_1} + \frac{m_2^2 u_2^2}{p_1^2}\right]}{A_3^2} +$$

$$\frac{-2C\,\frac{\gamma-1}{\gamma+1}\,\frac{m_1^2}{p_1^2} + \frac{2 m_1 m_2}{p_1 p_1} + \frac{m_2^2}{p_1^2}}{A_3^2}$$

$$\frac{p_3}{p_1} = \frac{1}{\gamma+1}\left[1 + \gamma\frac{A_1 M_1^2 + A_2 M_2^2}{A_3}\right] \pm$$

$$\sqrt{\frac{\gamma^2}{(\gamma+1)^2}\left[1 + \gamma\frac{A_1 M_1^2 + A_2 M_2^2}{A_3}\right]^2 - \gamma^2 a^{*2}\left[\frac{A_1 M_1^2}{u_1 A_3} + \frac{A_2 M_2^2}{u_2 A_3}\right]^2}$$

(8) $$\frac{p_3}{p_1} = \frac{1+\gamma\left\{\frac{A_1 M_1^2 + A_2 M_2^2}{A_3}\right\}}{\gamma+1} \pm$$

$$\gamma\sqrt{\left[\frac{1+\gamma\frac{A_1 M_1^2 + A_2 M_2^2}{A_3}}{\gamma+1}\right]^2 - \left[\frac{A_1 M_1^2 \frac{a^*}{u_1} + A_2 M_2^2 \frac{a^*}{u_2}}{A_3}\right]^2}$$

From ⑥, the relation $C = \frac{\gamma+1}{2(\gamma-1)} a^{*2}$, and dividing by p_1,

$$u_3 = -\frac{\gamma}{\gamma-1}\cdot\frac{p_3}{p_1}\cdot\frac{p_1(1+A_2/A_1)}{p_1u_1+p_2u_2A_2/A_1} + \sqrt{\left(\frac{\gamma}{\gamma-1}\right)^2\left(\frac{p_3}{p_1}\right)^2\left(\frac{p_1(1+A_2/A_1)}{p_1u_1+p_2u_2A_2/A_1}\right)^2 + \frac{\gamma+1}{\gamma-1}a^{*2}}$$

$$u_3 = -\frac{\gamma}{\gamma-1}\frac{p_3}{p_1}\frac{1+A_2/A_1}{\frac{M_1^2}{u_1}+\frac{M_2^2}{u_2}\frac{A_2}{A_1}} + \sqrt{\left(\frac{1}{\gamma-1}\right)^2\left(\frac{p_3}{p_1}\right)^2\left(\frac{1+A_2/A_1}{\frac{M_1^2}{u_1}+\frac{M_2^2}{u_2}\frac{A_2}{A_1}}\right)^2 + \frac{\gamma+1}{\gamma-1}a^{*2}}$$

⑨
$$\frac{u_3}{a^*} = -\frac{1}{\gamma-1}\frac{p_3}{p_1}\frac{1+A_2/A_1}{\frac{M_1^2}{u_1/a^*}+\frac{M_2^2}{u_2/a^*}} + \sqrt{\frac{1}{(\gamma-1)^2}\left(\frac{p_3}{p_1}\right)^2\left(\frac{1+A_2/A_1}{\frac{M_1^2}{u_1/a^*}+\frac{M_2^2A_2/A_1}{u_2/a^*}}\right)^2 + \frac{\gamma+1}{\gamma-1}}$$

$$\frac{a^*}{u} = \sqrt{\frac{\gamma - 1 + 2/M^2}{\gamma + 1}}$$

$$\frac{p_3}{p_1} = \frac{1 + \gamma \dfrac{M_1^2 A_1 + M_2^2 A_2}{A_3}}{\gamma + 1} +$$

$$\gamma \sqrt{\left[\frac{1 + \gamma \dfrac{M_1^2 A_1 + M_2^2 A_2}{A_3}}{1 + \gamma}\right]^2 - \left[\frac{M_1^2 A_1 \sqrt{\dfrac{2}{M_2^2} + \gamma - 1} + M_2^2 A_2 \sqrt{\dfrac{2}{M^2} + \gamma - 1}}{\sqrt{\gamma + 1}\ A_3}\right]^2}$$

$$\frac{p_3}{p_1} = \frac{1 + \gamma \left\{ \dfrac{M_1^2 + M_2^2 A_2/A_1}{1 + A_2/A_1} \right\}}{1 + \gamma} \pm$$

$$\gamma \sqrt{\left[\frac{1 + \gamma \dfrac{M_1^2 + M_2^2 A_2/A_1}{1 + A_2/A_1}}{\gamma + 1}\right]^2 - \left[\frac{M_1^2 \dfrac{a^*}{u_1} + M_2^2 \dfrac{A_2}{A_1} \dfrac{a^*}{u_2}}{1 + A_2/A_1}\right]^2}$$

(10) $$p_4/p_3 = \left(1 + \frac{\gamma - 1}{2} M_3^2\right)^{\frac{\eta \gamma}{\gamma - 1}}$$

η = diffuser efficiency

$$p_1/p_0 = \frac{1}{\left(1 + \dfrac{\gamma - 1}{2} M_1^2\right)^{\frac{\gamma}{\gamma - 1}}}$$

$$p_4/p_0 = p_4/p_3 \cdot p_3/p_1 \cdot p_1/p_0 \equiv 1 \quad \text{(design)}$$

(11) $$p_3/p_1 = p_0/p_1 \cdot p_3/p_4 = \frac{p_0/p_1}{p_4/p_3} = \frac{\left(1+\frac{\gamma-1}{2}M_1^2\right)^{\frac{\gamma}{\gamma-1}}}{\left(1+\frac{\gamma-1}{2}M_3^2\right)^{\frac{\gamma}{\gamma-1}}}$$

p_5/p_0, or λ, may be found from the following relations;

$$p_0/p_1 = \left(1+\frac{\gamma-1}{2}M_1^2\right)^{\frac{\gamma}{\gamma-1}}$$

$$p_5/p_1 = \left(1+\frac{\gamma-1}{2}M_2^2\right)^{\frac{\gamma}{\gamma-1}}$$

$$\therefore \lambda = \left[\frac{1+\frac{\gamma-1}{2}M_2^2}{1+\frac{\gamma-1}{2}M_1^2}\right]^{\frac{\gamma}{\gamma-1}}$$

The parameters may now be reduced by one by representing any combination of M_1 and M_2 by λ.

Design curves may now be drawn showing λ vs. p_4/p_0 for various values of A_2/A_1 at different values of M_1.

Since;

$$a^{*2} = \frac{2}{\gamma+1} \gamma R T_0 \text{, and}$$

$$\left(\frac{u}{a^*}\right)^2 = \frac{\gamma+1}{\gamma-1+\frac{2}{M^2}} \text{,}$$

a plot can be made showing u/a^* vs. M, see Fig.

Then by assuming a pair of values for M_1 and M_2, equation (8) is evaluated. Using these results in equation (9) gives values for u_3/a^*, giving M_3.

The value for M_3 gives a value for p_4/p_3: equation (10). Applying this to (11), p_4/p_0 is obtained, and these curves are shown in Fig. 1A

Calculation of Friction Losses

Working Section, 12" x 2.5" x 42"

Assuming $T_o = 540°F.$ abs., an M of 0.96 in the working section, and a characteristic length of 2.5', R = 12,000,000, and $C_f = 0.0025$

$$\Delta p A = C_f \cdot S \cdot q = f$$

$$q = \tfrac{1}{2} \cdot \frac{0.002378}{144} \cdot 64 \cdot 1000^2 = 5.28 \text{ p.s.i.}$$

$$S = 42" \times 29" = 1220 \text{ ins.}^2$$

$$A = 2.5" \times 12" = 30 \text{ ins.}^2$$

$$\Delta p_1 = \frac{0.0025 \times 1220 \times 5.28}{30} = 0.54 \text{ p.s.i.}$$

Mixing Section, 12" x 12" x 2.58"

Approximately one half of this area will be subjected to Mach numbers higher than one, say two, and q may average 15 p.s.i. Then, as above,

$$\Delta p_2 = \frac{0.002 \times 350 \times 15}{31} = 0.339 \text{ p.s.i.}$$

The total Δp in working and mixing sections $= 0.54 + 0.339 = 0.88$ p.s.i., and the friction loss $= \frac{0.88}{14.7} \doteq 0.05$

In order to take this into account, p_4/p_0 is considered at a value of 1.05. The diffuser loss is represented by $\eta = 75\%$ in the equations.

Fig. 1-B is plotted from Fig. 1-A as follows:—

the intersections of the curves of 1-A with a p_4/p_0 value of 1.05 give values of λ vs. M for each A_2/A_1. Corresponding values of A_1/A_3 are then plotted on 1-B

Figs. 1-C, D, E, and F are self-explanatory and were used in the calculations which are appended to this section.

INDUCTION OPERATION PERFORMANCE CALCULATIONS

$\gamma = 1.405$

(1)	(2)	(3)	(4)	(5)	(6)	(7)	(8)
M_1=0.8 Assumed	M_2 Assumed	$\frac{ps/p_1}{f(M_2)}$	λ=ps/po (3)/(24)	$\frac{A_2/A_j}{f(M_2)}$	A_j/A_3 Assumed	A_2/A_3 (5) (6)	A_1/A_3 1- (7)
	1.4	3.20	2.10	1.10	.09	.099	.901
	1.4	3.20	2.10	1.10	.06	.066	.934
	1.4	3.20	2.10	1.10	.03	.033	.967
	1.6	4.29	2.814	1.23	.09	.1107	.889
	1.6	4.29	2.814	1.23	.06	.0738	.9262
	1.6	4.29	2.814	1.23	.03	.0369	.9631
	1.8	5.81	3.81	1.42	.09	.1278	.8722
	1.8	5.81	3.81	1.42	.06	.0851	.9149
	1.8	5.81	3.81	1.42	.03	.0426	.9574
	2.0	7.87	5.16	1.67	.09	.150	.850
	2.0	7.87	5.16	1.67	.06	.100	.90
	2.0	7.87	5.16	1.67	.03	.051	.949
M_1= 0.6 Assumed	1.4	3.20	2.506	1.10	.09	.099	.901
	1.4	3.20	2.506	1.10	.06	.066	.934
	1.4	3.20	2.506	1.10	.03	.033	.967
	1.4	3.20	2.506	1.10	.01	.011	.989
	1.6	4.29	3.36	1.23	.09	.1107	.8893
	1.6	4.29	3.36	1.23	.06	.0738	.9262
	1.6	4.29	3.36	1.23	.03	.0369	.9631
	1.6	4.29	3.36	1.23	.01	.0123	.9877
	1.8	5.81	4.55	1.42	.09	.1278	.8722
	1.8	5.81	4.55	1.42	.06	.0851	.9149
	1.8	5.81	4.55	1.42	.03	.0426	.9574
	1.8	5.81	4.55	1.42	.01	.0142	.9858
	2.0	7.87	6.165	1.67	.09	.150	.850
	2.0	7.87	6.165	1.67	.06	.100	.900
	2.0	7.87	6.165	1.67	.03	.051	.949
	2.0	7.87	6.165	1.67	.01	.0167	.9833
M_1= 0.4 Assumed	1.4	3.20	2.864	1.10	.09	.099	.910
	1.4	3.20	2.864	1.10	.06	.066	.934
	1.4	3.20	2.864	1.10	.03	.033	.967
	1.6	4.29	3.84	1.23	.09	.1107	.8893
	1.6	4.29	3.84	1.23	.06	.0738	.9262
	1.6	4.29	3.84	1.23	.03	.0369	.9631
	1.8	5.81	5.20	1.42	.09	.1278	.8722
	1.8	5.81	5.20	1.42	.06	.0851	.9149
	1.8	5.81	5.20	1.42	.03	.0426	.9574
	2.0	7.87	7.05	1.67	.09	.150	.850
	2.0	7.87	7.05	1.67	.06	.100	.900
	2.0	7.87	7.05	1.67	.03	.051	.949

SUPERSONIC JET

	(9) $(1)^2(8)$	(10) $(2)^2(7)$	(11) (9)+(10)	(12) γ(11)	(13) $\frac{1+(12)}{1+\gamma}$	(14) $(13)^2$	(15) u_1/a^* $f(M_1)$	(16) u_2/a^* $f(M_2)$
0.8	.577	.194	.771	1.083	.865	.750		1.296
	.597	.1292	.7262	1.020	.939	.703		1.296
	.619	.0647	.6837	.960	.815	.666		1.296
	.569	.284	.853	1.198	.911	.831		1.42
	.593	.189	.782	1.100	.8715	.760		1.42
	.6165	.0945	.7105	.999	.830	.690	0.83	1.42
	.558	.414	.972	1.366	.982	.965		1.53
	.585	.276	.861	1.210	.917	.841		1.53
	.613	.138	.751	1.055	.851	.726		1.53
	.544	.600	1.144	1.608	1.082	1.174		1.626
	.576	.400	.976	1.371	.9845	.970		1.626
	.607	.200	.807	1.133	.885	.785		1.626
0.6	.3242	.194	.5182	.727	.7165	.514		1.296
	.336	.1292	.4652	.6545	.687	.472		1.296
	.348	.0647	.4127	.580	.6555	.430		1.296
	.356	.02156	.37756	.530	.635	.404		1.296
	.320	.2836	.6036	.848	.767	.589		1.42
	.3336	.189	.5226	.735	.720	.5195		1.42
	.3464	.0945	.4409	.620	.6725	.453	0.63	1.42
	.3564	.0315	.3879	.545	.641	.411	0.63	1.42
	.314	.414	.728	1.022	.840	.706		1.53
	.329	.276	.605	.850	.7685	.590		1.53
	.3446	.38	.4826	.6785	.696	.485		1.53
	.3552	.046	.4012	.564	.650	.4235		1.53
	.306	.600	.906	1.272	.943	.890		1.626
	.324	.400	.724	1.016	.8365	.700		1.626
	.3416	.200	.5416	.761	.731	.536		1.626
	.354	.0668	.4208	.5915	.661	.438		1.626
0.4	.144	.194	.338	.475	.6125	.3755		1.296
	.1491	.1292	.2783	.3914	.5785	.335		1.296
	.1547	.0647	.2194	.3082	.543	.295		1.296
	.142	.2836	.4256	.5985	.663	.440		
	.142	.2836	.4256	.5985	.663	.440		1.42
	.148	.189	.337	.474	.612	.375		1.42
	.154	.0945	.2485	.3494	.560	.314	0.43	1.42
	.1394	.414	.5534	.778	.738	.545		1.53
	.1461	.276	.4221	.5925	.661	.438		1.53
	.1531	.138	.2911	.409	.585	.3425		1.53
	.136	.600	.736	1.034	.845	.714		1.626
	.144	.400	.544	.764	.7325	.538		1.626
	.1518	.200	.3518	.494	.620	.385		1.626

	(17) (9)/(15)	(18) (10)/(16)	(19) (7)+(18)	(20) $(19)^2$	(21) $\sqrt{(14)-(20)}$	(22) $\sqrt{(21)}$	(23) $\frac{p3}{p1}$ (13)+(22)	(24) $\frac{p0}{p1}$ $f(M_1)$
0.8	.695	.1495	.8445	.712	.195	.274	1.130	
	.719	.0996	.8186	.670	.1816	.2552	1.0942	
	.745	.0499	.7949	.631	.187	.2628	1.0778	
	.685	.200	.885	.784	.2166	.3044	1.2154	
	.714	.133	.847	.719	.2024	.2844	1.1559	
	.742	.0665	.8085	.653	.1922	.270	1.100	1.525
	.671	.270	.941	.888	.2774	.390	1.372	
	.7045	.1803	.8848	.783	.2406	.338	1.255	
	.7385	.0901	.8386	.686	.200	.281	1.132	
	.655	.369	1.024	1.05	.352	.495	1.577	
	.694	.246	.940	.884	.2932	.412	1.3965	
	.731	.123	.854	.730	.2342	.3296	1.2146	
0.6	.515	.1496	.6646	.440	.272	.382	1.0985	
	.533	.0996	.6326	.400	.2682	.3768	1.0638	
	.5525	.0499	.6024	.363	.2586	.3636	1.0191	
	.5645	.01162	.58112	.338	.2568	.3606	..9956	
	.508	.1996	.7076	.500	.2982	.4195	1.1865	
	.529	.133	.662	.439	.2838	.3982	1.1182	
	.550	.0665	.6165	.380	.270	.3794	1.0519	
	.5655	.02218	.58768	.345	.2568	.3606	1.0016	1.276
	.4985	.2704	.7689	.590	.3402	.478	1.318	
	.522	.1803	.7023	.494	.3098	.435	1.2035	
	.547	.0901	.6371	.4055	.282	.396	1.092	
	.5635	.03006	.59356	.3525	.2664	.3742	1.0242	
	.4855	.369	.8545	.730	.400	.5620	1.5050	
	.5145	.246	.7605	.580	.3462	.4865	1.3230	
	.542	.123	.665	.442	.3064	.4305	1.1615	
	.562	.04105	.60305	.364	.272	.382	1.043	
0.4	.3346	.1496	.4842	.234	.376	.528	1.1405	
	.3466	.0955	.4421	.1956	.3734	.5245	1.1030	
	.3598	.0499	.4097	.168	.356	.514	1.057	
	.330	.1996	.5296	.280	.400	.5620	1.223	
	.344	.133	.477	.2275	.384	.540	1.152	1.1167
	.358	.0665	.4245	.180	.366	.514	1.074	
	.324	.2704	.5944	.353	.438	.615	1.353	
	.340	.1803	.5203	.271	.4085	.574	1.235	
	.356	.0901	.4461	.199	.3782	.5315	1.1165	
	.316	.369	.685	.470	.494	.694	1.1539	
	.3346	.246	.5806	.3375	.448	.629	1.3615	
	.3526	.123	.4256	.2265	.398	.559	1.179	

	(25)	(26)	(27)	(28)	(29)	(30)	(31)	(32)
	p_3/p_o (23)/(24)	A_2/A_1	$\frac{1}{1-\nu}$	1 + (26)	$(1)^2/(14)$	$(2)^2/(15)$	(30)(26)	(29)+(31)
0.8	.745	.1099		1.1099		1.512	.166	.937
	.716	.0707		1.0707		1.512	.107	.878
	.705	.03417		1.0342		1.512	.05165	.823
	.7955	.1245		1.1245		1.802	.2245	.995
	.757	.07975	-2.48	1.0798		1.802	.1440	.915
	.7205	.03836		1.0384	.771	1.802	.0692	.840
	.900	.1467		1.1467		2.118	.3103	1.081
	.822	.0925		1.0925		2.118	.1960	.967
	.742	.0444		1.0444		2.118	.0940	.865
	1.033	.1765		1.1765		2.460	.434	1.205
	.915	.1111		1.1111		2.460	.2736	1.045
	.795	.0538		1.0538		2.460	.1326	.904
0.6	.860	.1099		1.1099		1.512	.166	.738
	.834	.0707		1.0707		1.512	.107	.679
	.798	.03417		1.03417		1.512	.05165	.624
	.780	.01112		1.01112		1.512	.016825	.589
	.929	.1245		1.1245		1.802	.2245	.797
	.875	.07975		1.07975		1.802	.1440	.716
	.8245	.03836	-2.48	1.03836	.572	1.802	.0692	.641
	.7845	.01247		1.01247		1.802	.02347	.594
	1.031	.1467		1.1467		2.118	.3103	.882
	.942	.0925		1.0925		2.118	.1960	.768
	.855	.0444		1.0444		2.118	.0940	.666
	.8015	.0144		1.0144		2.118	.0305	.602
	1.178	.1765		1.1765		2.460	.434	1.006
	1.036	.1111		1.1111		2.460	.2736	.846
	.91	.0538		1.0538		2.460	.1326	.705
	.8165	.0170		1.0170		2.460	.0418	.614
0.4	1.02	.1099		1.1099		1.512	.166	.538
	.986	.0707		1.0707		1.512	.107	.479
	.945	.03417		1.0342		1.512	.05165	.424
	1.094	.1245		1.1245		1.802	.2245	.597
	1.03	.07975	-2.48	1.0798		1.802	.1440	.516
	.960	.03836		1.0384		1.802	.0692	.441
	1.21	.1467		1.1467	.372	2.118	.3103	.682
	1.105	.0925		1.0925		2.118	.1960	.568
	1.000	.0444		1.0444		2.118	.0940	.466
	1.377	.1765		1.1765		2.460	.434	.806
	1.219	.1111		1.1111		2.460	.2736	.646
	1.054	.0538		1.0538		2.460	.1326	.505

	(33)	(34)	(35)	(36)	(37)	(38)	(39)	(40)
	$\frac{(28)(22)(27)}{(32)}$	(33)2	$\sqrt{(34)+6}$	u_3/a^* (33)+(35)	M_3^2 f(36)	1+.2015(37)	p^4/p^3 $(39)^{2.61}$	p^4/p_o (39)(25)
= 0.8	3.345	11.18	4.145	.800	.598	1.1206	1.346	1.002
	3.311	10.96	4.118	.807	.608	1.1235	1.356	.971
	3.359	11.28	4.157	.798	.593	1.1196	1.343	.947
	3.407	11.60	4.195	.788	.578	1.1164	1.334	1.062
	3.383	11.42	4.173	.790	.578	1.1164	1.334	1.011
	3.370	11.36	4.166	.796	.592	1.1192	1.342	.967
	3.608	13.02	4.361	.753	.521	1.1050	1.298	1.168
	3.515	12.36	4.285	.770	.548	1.1105	1.315	1.081
	3.389	11.48	4.181	.792	.581	1.1171	1.336	.991
	3.818	14.57	4.536	.718	.468	1.0944	1.266	1.309
	3.683	13.56	4.423	.740	.501	1.1010	1.286	1.178
	3.511	12.33	4.282	.771	.549	1.1107	1.315	1.046
= 0.6	-4.096	16.77	4.771	.675	.409	1.0824	1.229	1.055
	-4.161	17.31	4.828	.667	.401	1.0808	1.225	1.021
	-4.190	17.56	4.854	.664	.397	1.08	1.222	.976
	-4.240	17.98	4.897	.657	.386	1.0777	1.216	.949
	-4.151	17.23	4.82	.669	.408	1.0822	1.229	1.141
	-4.182	17.49	4.847	.665	.397	1.08	1.222	1.070
	-4.225	17.85	4.884	.659	.387	1.078	1.217	1.002
	-4.234	17.92	4.891	.657	.386	1.0778	1.216	.954
	-4.256	18.11	4.910	.654	.384	1.0774	1.215	1.253
	-4.246	18.03	4.902	.656	.385	1.0776	1.215	1.144
	-4.247	18.04	4.903	.656	.385	1.0776	1.215	1.039
	-4.280	18.32	4.932	.652	.384	1.0774	1.215	.974
	-4.366	19.06	5.006	.640	.367	1.074	1.215	1.431
	-4.309	18.56	4.956	.647	.378	1.0762	1.211	1.257
	-4.305	18.53	4.953	.648	.378	1.0762	1.211	1.103
	-4.286	18.37	4.937	.651	.384	1.0774	1.215	.993
= 0.4	-5.836	34.05	6.329	.493	.210	1.0423	1.114	1.137
	-6.222	38.71	6.687	.465	.185	1.0373	1.100	1.085
	-6.392	40.85	6.845	.453	.176	1,0354	1.095	1.035
	-5.712	32.63	6.215	.503	.221	1.0445	1.120	1.226
	-5.979	35.75	6.462	.483	.203	1.0409	1.110	1.142
	-6.272	39.33	6.733	.461	.183	1.0369	1.099	1.053
	-5.639	31.80	6.148	.509	.228	1.0459	1.124	1.361
	-5.891	34.71	6.381	.490	.210	1.0423	1.114	1.22
	-6.205	38.50	6.666	.461	.182	1.0366	1.098	1,098
	-5.574	31.07	6.089	.515	.230	1.0463	1.125	1.55
	-5.808	33.74	6.304	.496	.212	1.0427	1.115	1.36
	-6.098	37.20	6.573	.475	.194	1.0391	1.105	1.165

ADDITIONAL CALCULATIONS - SUPERSONIC JET THEORY

NOTE: For $M_1 = 1.0$ a slightly modified form of carrying out the calculations was used in order to check the form used for $M_1 = 0.4$, 0.6 and 0.8. The smoothness of the curves testifies as to the accuracy of both methods.

The condensed results of this calculation are:

$M_1 = 1$

	A_2/A_1 (=R)	p_3/p_1	u_3/a^*	M_3	p_4/p_3	p_3/p_o	p_4/p_o
3	.08	1.338	.854	.83	1.373	.730	1.004
	.07	1.291	.871	.85	1.426	.682	.972
	.06	1.265	.879	.86	1.437	.664	.961
	.05	1.244	.884	.863	1.440	.658	.947
	.04	1.2027	.901	.882	1.462	.635	.929
4	.08	1.423	.830	.800	1.373	.753	1.034
	.07	1.380	.838	.814	1.387	.730	1.011
	.06	1.3466	.849	.824	1.398	.711	.994
	.05	1.2925	.869	.845	1.420	.684	.972
	.04	1.2574	.879	.860	1.436	.664	.953
5	.08	1.4982	.805	.780	1.352	.793	1.071
	.07	1.436	.830	.800	1.373	.759	1.042
	.06	1.399	.839	.815	1.387	.740	1.025
	.05	1.346	.850	.825	1.399	.711	.994
	.04	1.314	.858	.835	1.409	.693	.976
6	.08	1.569	.778	.750	1.322	.829	1.096
	.07	1.506	.802	.770	1.350	.796	1.075
	.06	1.464	.810	.780	1.352	.775	1.048
	.05	1.407	.830	.800	1.373	.742	1.020
	.04	1.34	.840	.820	1.392	.709	.988

Sonic Jet Calculations

(1) M_1	(2) u_1/a^* $f(M_1)$	(3) p_1/p_o $f(M_1)$	(4) Assume (p_s/p_o)	(5) p_2/p_s	(6) A_2/A_3	(7) A_1/A_3 $1-(6)$	(8) $\frac{p_2/p_1}{(5)(4)/(3)}$	(9) $1+\gamma(1)^2$	(10) $(7)(9)$	(11) $(1+\gamma)(6)(8)$
0.4	.43	.895	2	.528	.05	.95	1.181	1.2245	1.1620	.1423
					.10	.90			1.1010	.2845
					.15	.85			1.0400	.4270
			3		.05	.95	1.771		1.162	.213
					.10	.90			1.101	.426
					.15	.85			1.040	.639
			4		.05	.95	2.361		1.162	.285
					.10	.90			1.101	.569
					.15	.85			1.040	.855
			6		.01	.99	3.54	1.2246	1.2110	.0851
					.04	.96			1.175	.3418
0.6	.63	.782	2	.528	.05	.95	1.35	1.5055	1.43	.1624
					.10	.90			1.355	.3248
			3		.05	.95	2.024		1.43	.2435
					.10	.90			1.355	.4870
					.15	.85			1.28	.7305
			4		.05	.95	2.70		1.43	.3250
					.10	.90			1.355	.6500
			2		.175	.825	1.35	1.505	1.241	.570
			4		.08	.92	2.70		1.383	.520
			7		.01	.99	4.74		1.489	.1140
					.03	.97			1.460	.342
					.05	.95			1.430	.570
0.8	.83	.657	3	.528	.05	.95	2.41	1.900	1.805	.2900
					.10	.90			1.71	.5800
					.15	.85			1.614	.8700
			4		.05	.95	3.218		1.805	.387
					.10	.90			1.71	.774
					.15	.85			1.614	1.161
			5		.05	.95	4.02		1.805	.4835
					.10	.90			1.71	.967
					.15	.85			1.614	1.4505
			9		.01	.99	7.22	1.900	1.880	.1736
					.03	.97			1.841	.5208
					.0					
0.95	.96	.562	3		.05	.95	2.82	2.267	2.17	.3395
					.10	.90			2.04	.6790
					.15	.85			1.925	1.0185
			4		.05	.95	3.76		2.17	.4525
					.10	.90			2.04	.905
					.15	.85			1.925	1.3575
			5		.05	.95	4.70	2.27	2.17	.565
					.10	.90			2.04	1.130
					.15	.85			1.925	1.695
					.12	.88	4.71		1.996	1.36
					.18	.82			1.86	2.04
			6.3		.06	.94	5.94		2.13	.857
					.12	.88			1.996	1.714
			4		.20	.80	3.758	2.267	1.813	1.807
			5		.01	.99	4.71	2.27	2.2460	.1132
					.08	.92			2.09	.9075
			4		.13	.87	3.77		1.972	1.180
			7		.08	.92	6.6		2.086	1.27
					.09	.91			2.064	1.429
					.10	.90			2.040	1.587

(12)	(13)	(14)	(15)	(16)	(17)	(18)	(19)	(20)
(10)+(11)	$(12)^2$	$\frac{1}{1+\gamma}(12)$	$(\frac{\gamma}{\gamma+1})^2(13)$	$\frac{(1)^2}{(2)}$	(7)(16)	(6)(8)	(17)+(18)	$(\gamma(19))^2$
1.3043	1.70	.5410	.5795	.372	.3534	.0591	.4125	.3360
1.3855	1.92	.5750	.6550		.3350	.1181	.4531	.4055
1.4670	2.15	.6085	.7330		.3160	.1773	.4933	.4800
1.375	1.89	.5700	.6450		.3534	.0886	.4420	.3860
1.527	2.33	.6355	.7945		.3350	.1771	.5121	.5190
1.679	2.815	.6960	.9590		.3160	.2658	.5818	.6700
1.447	2.09	.6000	.7120		.3534	.1181	.4715	.4400
1.670	2.79	.6930	.9520		.3350	.2361	.5711	.6450
1.895	3.60	.7860	1.2280		.3160	.3543	.6703	.8900
1.2961	1.68	.537	.673		.3580	.0354	.3934	.306
1.516	2.30	.6285	.7845		.3550	.1416	.4966	.4885
1.5924	2.54	.661	.865	.571	.542	.0675	.6095	.232
1.6798	2.82	.697	.961		.514	.135	.649	.831
1.6735	2.80	.965	.955		.542	.1012	.6432	.818
1.8420	3.40	.765	1.16		.514	.2024	.7164	1.014
2.0105	4.05	.934	1.382		.485	.3036	.7886	1.24
1.7550	3.085	.728	1.053		.542	.135	.677	.907
2.0050	4.035	.8325	1.376		.514	.270	.784	1.214
1.903	3.625	.789	1.248		.525	.216	.741	1.084
1.811	3.28	.752	1.119		.4715	.2361	.7076	.99
1.603	2.575	.665	.8775		.565	.474	.6124	.740
1.802	3.250	.7475	1.109		.554	.1422	.6962	.959
2.000	4.000	.830	1.364		.542	.2370	.7790	1.200
2.095	4.39	.869	1.498	.771	.7325	.1205	.853	1.438
2.29	5.25	.95	1.79		.694	.241	.935	1.726
2.484	6.19	1.031	2.11		.655	.3615	1.0165	2.04
2.192	4.80	.91	1.638		.7325	.1609	.8934	1.575
2.484	6.18	1.031	2.108		.694	.3218	1.0158	2.04
2.775	7.70	1.150	2.622		.655	.4827	1.1377	2.555
2.2885	5.24	.95	1.787		.7325	.201	.9335	1.72
2.677	7.17	1.110	2.446		.694	.402	1.096	2.375
3.0645	9.40	1.271	3.204		.655	.603	1.258	3.13
2.054	4.215	.852	1.439		.7635	.0722	.8352	1.380
2.362	5.59	.980	1.907		.748	.2166	.9646	1.840
2.510	6.3	1.04	2.15	.941	.894	.141	1.035	2.115
2.719	7.39	1.128	2.52		.846	.282	1.128	2.51
2.943	8.68	1.221	2.96		.8	.423	1.223	2.955
2.6225	6.9	1.089	2.352		.894	.188	1.082	2.315
2.945	8.69	1.222	2.96		.846	.376	1.222	2.95
3.283	10.78	1.363	3.68		.8	.564	1.364	3.68
2.735	7.49	1.135	2.552		.894	.235	1.129	2.515
3.17	1.003	1.317	3.42		.846	.470	1.316	3.42
3.62	13.1	1.502	4.465		.8	.705	1.505	4.48
3.36	11.3	1.394	3.856	.938	.825	.565	1.390	3.815
3.90	15.2	1.618	5.185		.764	.8475	1.6165	5.16
2.987	8.91	1.24	3.04		.88	.356	1.236	3.02
*3.710	13.8	1.54	4.70		.825	.712	1.537	4.66
2.3592	5.56	.976	1.895		.9385	.0471	.9756	1.880
2.9975	9.00	1.243	3.07		.8630	.3766	1.2396	3.05
3.152	9.94	1.309	3.388	.940	.8175	.4900	1.3075	3.375
3.356	11.26	1.382	3.840	.938	.862	.528	1.390	3.815
3.493	12.20	1.450	4.160		.8535	.594	1.4475	4.140
3.627	13.16	1.506	4.485		.8445	.660	1.5045	4.465
*3.620	13.15	1.502	4.48	.941	.7528	.7516	1.5044	4.47

(21) (15)-(20)	(22) $\sqrt{(21)}$	(23) p_3/p_1 (14)+(22)	(24) A_2/A_1 (6)/(7)	(25) 1 + (24)	(26) (16)+(24)	(27) $-\frac{1}{\gamma-1}\frac{(23)(25)}{(26)}$	(28) $(27)^2+\frac{\gamma+1}{\gamma-1}$
.2435	.4935	1.0345	.05265	1.05265	.4246	-6.345	46.14
.2495	.4995	1.0745	.11111	1.11111	.483	-6.110	43.29
.2530	.5030	1.1115	.17650	1.17650	.549	-5.890	40.59
.2590	5085	1.0785	.05265	1.05265	.4246	-6.610	49.69
.2755	.5250	1.1605	.11111	1.11111	.483	-6.600	49.54
.2890	.5370	1.2330	.17650	1.17650	.549	-6.525	49.84
.2720	.5215	1.1215	.05265	1.05265	.4246	-6.899	53.44
.3070	.5545	1.2475	.11111	1.11111	.483	-7.090	56.04
.3380	.5810	1.3670	.17650	1.17650	.549	-7.235	58114
.3670	.605	1.142	.0101	1.0101	.3821	-7.45	61.54
.2960	.5440	1.1725	.04165	1.04165	.41365	-7.30	59.24
.133	.362	1.023	.05265	1.05265	.6237	-4.27	24.16
.130	.3602	1.0562	.11111	1.11111	.6821	-4.255	24.08
.137	.37	1.065	.05265	1.05265	.6237	-4.440	25.64
.146	.382	1.147	.11111	1.11111	.6824	-4.615	27.24
.142	.3764	1.2104	.17650	1.17650	.7475	-4.710	28.14
.146	.382	1.110	.05265	1.05265	.6237	-4.640	27.44
.162	.4025	1.235	.11111	1.11111	.6821	-4.975	30.74
.164	.405	1.194	.087	1.087	.658	-4.87	29.69
.129	.359	1.111	.212	1.212	.783	-4.25	24.07
.1375	.3705	1.0355	.0101	1.0101	.5811	-4.45	25.74
.150	.3872	1.1347	.03094	1.03094	.60194	-4.80	29.00
.164	.4050	1.235	.0527	1.0526	.6236	-5.15	32.44
.060	.2448	1.1138	.05265	1.05265	.82365	-3.570	18.70
.064	.2528	1.2028	.11111	1.11111	.8821	-3.750	20.02
.070	.2646	1.2956	.17650	1.17650	.9475	-3.966	21.68
.063	.2508	1.1608	.05265	1.05265	.82365	-3.66	19.34
.068	.2608	1.2918	.11111	1.11111	.8821	-4.080	22.14
.067	.2588	1.4088	.17650	1.17650	.9475	-4.315	24.56
.067	.2586	1.2086	.05265	1.05265	.82365	-3.820	20.54
.071	.2662	1.3762	.11111	1.11111	.8821	-4.235	23.90
.074	.272	1.543	.17650	1.17650	.9475	-4.735	28.34
.059	.2428	1.0948	.0101	1.0101	.7811	-3.50	18.18
.067	.2587	1.2387	.03094	1.03094	.80194	-3.936	21.45
.035	.187	1.227	.05275	1.05265	.99365	-3.212	16.26
.01	.1	1.228	.11111	1.11111	1.0521	-3.204	16.22
.005	.077	1.298	.17650	1.17650	1.1175	-3.37	17.32
.037	.1922	1.2812	.05265	1.05265	.99365	-3.356	17.20
.01	.1	1.322	.11111	1.11111	1.0521	-3.448	17.84
.0	0	1.363	.17650	1.17650	1.1175	-3.544	18.54
.037	.1921	1.3271	.05265	1.05265	.99365	-3.479	18.04
0	0	1.317	.11111	1.11111	1.0521	-3.436	17.74
0	0	1.502	.17650	1.17650	1.1175	-3.91	21.24
.041	.202	1.596	.1363	1.1363	.7073	-6.33	46.
.025	.158	1.776	.2196	1.2196	.7906	-6.75	52.5
.02	.1414	1.3814	.0638	1.0638	.6358	-5.725	38.74
.04	.2000	1.74	.1363	1.1363	.7073	-6.900	53.54
.01	.10	1.602	.25	1.25	1.1191	-4.15	23.18
.015	.1224	1.0984	.0101	1.0101	.9481	-2.89	14.31
.02	.1414	1.3844	.0870	1.087	1.025	-3.626	19.14
.013	.114	1.423	.1494	1.1494	1.0894	-3.702	19.68
.035	.1870	1.5690	.0970	1.0970	1.0350	-4.110	22.84
.020	.1414	1.5914	.0989	1.0989	1.0369	-4.165	23.28
.020	.1414	1.6464	.1111	1.1111	1.0491	-4.310	24.54

(29)	(30)	(31)	(32)	(33)	(34)	(35)
$\sqrt{(28)}$	u_3/a^* (27)+(29)	M_3 f(30)	$1+.2015(31)^2$	p_4/p_3 $(32)^{2.61}$	p_3/p_o (23)(3)	p_4/p_o (33)(34)
6.795	.450	.42	1.0355	1.0954	.925	1.012
6.580	.470	.434	1.0380	1.1022	.961	1.060
6.370	.480	.445	1.0399	1.1075	.996	1.103
7.050	.440	.404	1.03290	1.0881	.964	1.048
7.045	.445	.412	1.03420	1.0919	1.039	1.134
7.060	.535	.500	1.0502	1.1363	1.102	1.255
7.310	.420	.388	1.0304	1.0811	1.003	1.085
7.490	.410	.380	1.0291	1.0777	1.116	1.201
7.820	.585	.552	1.0615	1.1685	1.221	1.427
7.84	.39	.364	1.0267	1.0711	1.022	1.096
7.70	.40	.370	1.0276	1.0736	1.05	1.130
4.915	.645	.61	1.0752	1.208	.8	.965
4.91	.655	.62	1.0777	1.2158	.826	1.004
5.065	.625	.592	1.0708	1.1955	.8325	.995
5.215	.600	.57	1.0657	1.1805	.896	1.059
5.305	.595	.56	1.0634	1.174	.946	1.111
5.235	.595	.56	1.0634	1.174	.868	1.02
5.555	.580	.544	1.0596	1.1643	.965	1.123
5.45	.58	.544	1.0596	1.163	.933	1.085
4.91	.66	.626	1.0793	1.220	.868	1.058
5.075	.625	.592	1.0706	1.195	.809	.965
5.385	.585	.550	1.0610	1.167	.8865	1.034
5.695	.545	.510	1.0524	1.1425	.965	1.111
4.322	.752	.72	1.1044	1.296	.732	.949
4.495	.745	.71	1.1016	1.2874	.79	1.017
4.65	.684	.65	1.0852	1.238	.851	1.053
4.40	.74	.71	1.1016	1.2874	.763	.981
4.705	.685	.65	1.0852	1.238	.851	1.053
4.96	.645	.61	1.0750	1.208	.925	1.117
4.535	.715	.682	1.094	1.2642	.7935	1.002
4.885	.650	.62	1.0776	1.2156	.904	1.098
5.32	.585	.55	1.061	1.167	.1014	1.184
4.26	.760	.73	1.1074	1.3054	.720	.940
4.63	.694	.66	1.0880	1.2462	.814	1.013
4.030	.818	.792	1.1264	1.364	.69	.9405
4.027	.823	.794	1.127	1.366	.69	.9415
4.16	.79	.76	1.1166	1.334	.73	.974
4.15	.794	.764	1.1176	1.3364	.72	.962
4.225	.777	.746	1.1121	1.3200	.7435	.981
4.3	.756	.726	1.1062	1.3016	.766	.9965
4.25	.77	.74	1.1104	1.326	.745	.988
4.21	.774	.74	1.1104	1.326	.741	.982
4.67	.76	.73	1.1074	1.305	.845	1.100
6.78	.45	.42	1.0355	1.095	.893	.978
7.25	.50	.47	1.0445	1.1204	.983	1.075
6.22	.50	.464	1.0434	1.117	.774	.864
7.315	.415	.384	1.0298	1.0796	.975	1.05
4.815	.665	.63	1.080	1.2222	.901	1.100
3.78	.89	.87	1.1524	1.448	.614	.889
4.370	.744	.71	1.1007	1.316	.775	1.018
4.430	.728	.695	1.0975	1.2746	.797	1.016
4.780	.67	.636	1.0815	1.227	.878	1.077
4.825	.66	.628	1.0794	1.2206	.891	1.089
4.955	.645	.610	1.0750	1.208	.921	1.113

APPENDIX (C)

REDUCTION OF BRITISH DATA

For purposes of comparison it was considered worthwhile to plot the performance of other induction type wind tunnels on our performance curves.

The only available reference which set forth performance data in sufficient detail for our purpose was the British R & M No. 1468. This R & M dealt with early experimentation with induction type wind tunnels of, unfortunately, a rather small size and circular in cross section. A later report, R & M No. 1853, dealt with a rectangular cross section, 6" x 2-3/4", with high pressure jets on the longer sides only. Unfortunately, very meager performance data was included.

The tunnels described in the above reports were at a considerable variance with our tunnel in the matter of area of mixing section. The design theory and actual construction of our tunnel requires a mixing section of constant area; the theory (evidently "constant pressure") upon which was based the construction of the British tunnels calls for a rapid expansion of cross-sectional area in the mixing chamber; furthermore, this expansion commences at the downstream end of their working section, a short distance ahead of their jets.

In view of these variations in construction, it is necessary to correct their performance data in order to compare it with our theoretical and actual performance curves. The substance of the correction lies in reducing their observed working section Mach number to fit the larger cross sectional area at their jets.

This was readily accomplished by means of the relation plotted on Fig. 5.1

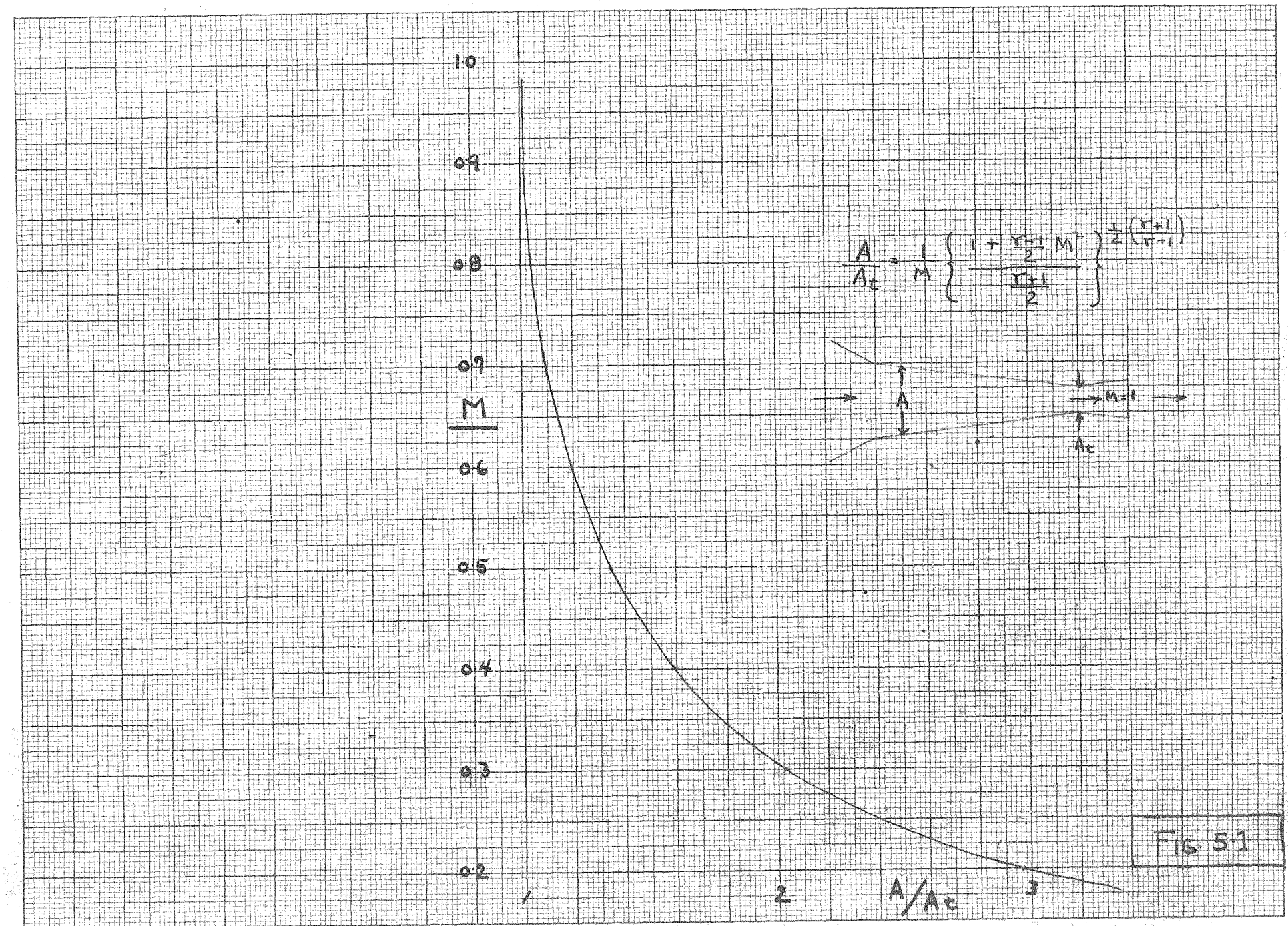
1·0
0·9
0·8
0·7
M
0·6
0·5
0·4
0·3
0·2
1
2
3
A/A*
$\frac{A}{A_t^*} = \frac{1}{M}\left\{\frac{1+\frac{\gamma-1}{2}M^2}{\frac{\gamma+1}{2}}\right\}^{\frac{1}{2}\left(\frac{\gamma+1}{\gamma-1}\right)}$
A
M=1
A*

Fig. 5·1

REDUCTION OF BRITISH DATA

(a) Ref: R & M No. 1468, Fig. 3, Curve F (0.020" annular nozzle)
Tunnel type - Circular, 2 1/4" diameter, annular nozzle

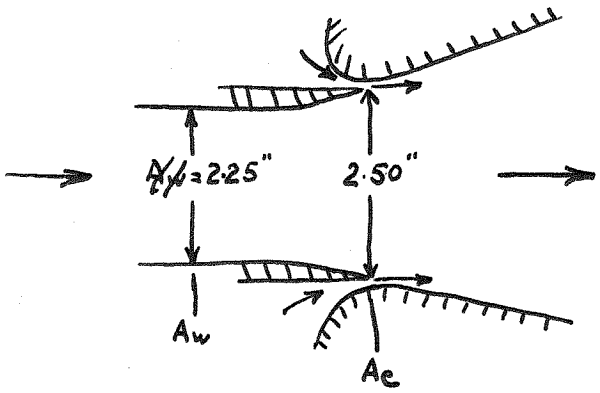

$$A_e = \frac{\pi}{4}(2.5)^2$$

$$A_w = \frac{\pi}{4}(2.25)^2$$

$$\frac{A_e}{A_w} = 1.24$$

$$\frac{A_j}{A_e} = \frac{2.5\pi \times .020}{\pi/4\ (2.5)^2} = .032$$

$$\frac{A_j}{A_e} = \frac{A_j}{A_3}$$

Mean Working Sec. Velocity fps	Nozzle Pressure psi abs.	λ (p = 14.7)	M_w	M_e	A_j/A_3
990	70	4.76	0.96	0.58	.032
910	60	4.08	0.882	0.545	.032
700	45	3.06	0.679	0.487	.032
600	38	2.59	0.582	0.439	.032
500	35	2.38	0.533	0.418	.032

(b) Ref: R & M No. 1853
Tunnel type - 6" x 2 3/4" working section; 2 jets, .045;

M = 0.96
Compression Ratio = 6.33
$A_w = 6 \times 2\ 3/4 = 16.5"^2$
$A_e = 6 \times 3 = 18"^2$
$A_j = 12 \times .045 = 0.54"^2$
$A_j/A_e = A_j/A_3 = 0.030$

Area Correction = $A_e/A_w = 1.09$

which gives $M_e = 0.69$